Personal Account

THE CHEMICAL RECORD

doi.org/10.1002/tcr.202300278
tcr.wiley-vch.de

A Personal Account on Inorganic Reaction Mechanisms

Justyna Polaczek,[a] Konrad Kieca,[a, b] Maria Oszajca,[a] Olga Impert,[d] Anna Katafias,[d] Debabrata Chatterjee,[d, e] Dušan Ćoćić,[f] Ralph Puchta,[c, g, h] Grażyna Stochel,[a] Colin D. Hubbard,[i] and Rudi van Eldik*[c, d]

Abstract: The presented Review is focused on the latest research in the field of inorganic chemistry performed by the van Eldik group and his collaborators. The first part of the manuscript concentrates on the interaction of nitric oxide and its derivatives with biologically important compounds. We summarized mechanistic information on the interaction between model porphyrin systems (microperoxidase) and NO as well as the recent studies on the formation of nitrosylcobalamin (CblNO). The following sections cover the characterization of the Ru(II)/Ru(III) mixed-valence ion-pair complexes, including Ru(II)/Ru(III)(edta) complexes. The last part concerns the latest mechanistic information on the DFT techniques applications. Each section presents the most important results with the mechanistic interpretations.

Keywords:

1. Introduction to Honoring Professor Dr. Rudi van Eldik

Professor van Eldik is well known to many in the Inorganic Chemistry academic research community especially those focusing on reaction mechanisms. A brief chemistry biography-journey follows. Rudi received his University-education at Potchefstroom University in South Africa, in the 1960s. He pursued postdoctoral research at the State University of New York in Buffalo, with Gordon Harris, followed by research with Hartwig Kelm in Frankfurt, leading to Habilitation, in 1982. Professorial calls to the Universities of Witten/Herdecke

[a] *J. Polaczek, K. Kieca, M. Oszajca, G. Stochel*
Faculty of Chemistry, Jagiellonian University, Gronostajowa 2, 30-387 Kraków, Poland
[b] *K. Kieca*
Jagiellonian University, Doctoral School of Exact and Natural Sciences, Kraków, 30-348 Krakow, Poland
[c] *R. Puchta, R. van Eldik*
Department of Chemistry and Pharmacy, University of Erlangen-Nuremberg, Egerlandstrasse 1, 91058 Erlangen, Germany
E-mail: rudi.vaneldik@fau.de
[d] *O. Impert, A. Katafias, D. Chatterjee, R. van Eldik*
Faculty of Chemistry, Nicolaus Copernicus University in Torun, Gagarina 7, 87-100 Torun, Poland
[e] *D. Chatterjee*
Vice-Chancellor's Research Group, Zoology Department, University of Burdwan, Burdwan-713104, India
[f] *D. Ćoćić*
University of Kragujevac, Faculty of Science, Department of Chemistry, Radoja Domanovića 12, P. O. Box 60, 34000 Kragujevac, Serbia
[g] *R. Puchta*
Central Institute for Scientific Computing (CISC), University of Erlangen-Nuremberg, Martensstr. 5a, 91058 Erlangen, Germany
[h] *R. Puchta*
Computer Chemistry Center, Department of Chemistry and Pharmacy, University of Erlangen-Nuremberg, Nägelsbachstr. 25, 91052 Erlangen, Germany
[i] *C. D. Hubbard*
Department of Chemistry, University of New Hampshire, Durham, 03824, USA

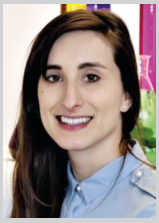

Justyna Polaczek was born in Nowy Targ, Poland, in 1990. In 2019 she received her PhD in the mechanism of nitrosylcobalamin formation, at Jagiellonian University, under the supervision of Prof. Rudi van Eldik. In 2019 she joined the research project at the Faculty of Chemistry, Jagiellonian University as a post-doctoral fellow and she studied the influence of air pollution on nitrosylcobalamin interactions. From 2021 she has been an Assistant Professor at the Faculty of Chemistry of the Jagiellonian University. Her research work focuses on the mechanistic and kinetic studies of bioinorganic processes, especially reactions of Vitamin B12's derivatives.

Konrad Kieca, born in Poland in 1997, pursued a double-degree program during his Master's studies, which included an internship in Orleans in Professor Stephane Petoud's research group. Currently, he is actively engaged in his PhD studies, working under the supervision of Professor Grażyna Stochel and Dr. Maria Oszajca within the Coordination and Bioinorganic Physicochemistry Group at the Jagiellonian University in Cracow. His primary research focus is centered on understanding the mechanisms of reactions that may have a significant impact on abnormalities in the cellular nitric oxide signaling pathway.

Maria Oszajca is an Assistant Professor at the Faculty of Chemistry of Jagiellonian University where she also obtained her PhD under the supervision of prof. Grażyna Stochel. During her research internships she worked in prof. Rudi van Eldik's group at the University of Erlangen-Nuremberg as well as in the group of prof. Claudine Kieda at CNRS Orléans. She has devoted her scientific career to study the chemical kinetics of various bioinorganic processes relevant to the internal workings of living organisms. Her particular interests lie in the activation mechanisms of small biorelevant molecules (NO, O_2, etc.) on iron-porphyrin model centers.

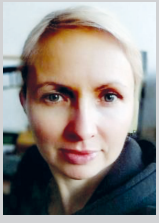

Olga Impert received her master's degree in 2001, and in 2007, the award of the Rector of the Nicolaus Copernicus University for her doctoral dissertation. In 2010, she did a post-doctoral fellowship with Prof. István Fábián from the University of Debrecen. She participated in a project co-financed by the European Union. She works in the team of Dr. A. Katafias and Prof. Rudi van Eldik. Currently, she studies the reactivity and catalytic activity of ruthenium(III) complexes in aqueous solutions. Synthesizing and characterizing novel Ru(II)/Ru(III) mixed-valence ion pairs is also a part of her research interest.

Anna Katafias obtained her PhD degree in chemistry (1999) and habilitation in chemistry (2013), speciality – inorganic and coordination chemistry, from the Nicolaus Copernicus University in Torun (Poland). She is currently an Associate Professor at the Faculty of Chemistry of her Alma Mater. Her research interests have centred on the elucidation of inorganic reaction mechanisms, in particular electron transfer processes, activation of small molecules, and homogeneous catalysis as well as the development of polypyridyl non-organometallic rutehnium(II) complexes as models for cellular redox modulation. Recently, her research has also included redox and ligand substitution reactions of nano- and microscale coordination compounds at the solid-liquid interface.

Dr. Debabrata Chatterjee is retired scientist and head of the Chemistry and Biomimetics Group, CSIR-Central Mechanical Engineering Research Institute at Durgapur, India. He is now engaged in Burdwan University as a research advisor. His current research interests lie in the kinetic and mechanistic studies of small molecule activation. His involvement in a broad range of research activities has resulted in 188 research papers and reviews in peer-reviewed journals. Childhood polio has left him physically challenged with a considerable mobility problem. He is fellow of the National Academy of Sciences (FNASc), India and Royal Society of Chemistry, UK (FRSC).

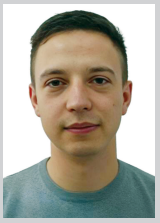

Dušan Ćoćić finished his Ph.D. in 2022 under the supervision of Biljana Petrovic at the University of Kragujevac in the field of Inorganic chemistry, more specifically in the field of experimental studied of bimetallic platinum(II) and palladium(II) complexes, their kinetic behaviour, and interactions with macromolecules. During his Ph.D. he joined the research group of Zivadin Bugarcic and Biljana Petrovic, and extended his research focus on quantum chemical calculation studies of mechanistic problems in chemistry. Currently he is a Research Associate at the Faculty of Science, University of Kragujevac.

After his Ph.D. in organic chemistry on a combined quantum chemical and experimental study in the field of supramolecular chemistry supervised by Tim Clark and Rolf W. Saalfrank, **Ralph Puchta** joined in 2004 the team of Rudi van Eldik at the Institute for Inorganic Chemistry in Erlangen, extending his research interest on computationally studies of mechanistic problems in coordination chemistry. Since 2013 he is Privatdozent at the Chair of Inorganic and Organometallic Chemistry in Erlangen, continuing his independent research and a number of national and international co-operations in inorganic and organic chemistry.

Grażyna Stochel is a Full Professor at the Inorganic Chemistry Department, Faculty of Chemistry, Jagiellonian University in Kraków, Poland. Leader of Coordination and Bioinorganic Physicochemistry Group. She is an ordinary member of the Polish Academy of Sciences and Academia Europaea. Her research field is Inorganic and Bioinorganic Chemistry, Coordination Chemistry, Photochemistry, Medicinal Chemistry, and Advanced Materials. Research activity is focused on: mechanisms of inorganic and bioinorganic reactions; photochemistry and photobiology of coordination compounds; catalysis and photocatalysis; activation of small inorganic molecules in biology, environment, and medicine; advanced inorganic materials and their use in innovative health and environmental protection strategies.

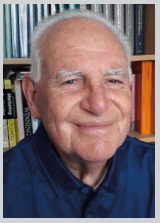

Colin D. Hubbard, received his tertiary chemistry education, culminating in a doctoral degree (1964) from the University of Sheffield, in the UK. He undertook postdoctoral research at MIT, Cornell University, and the University of California, Berkeley. In 1967 he joined the Chemistry Department of the University of New Hampshire, as Assistant Professor, Associate 1972 and Full Professor in 1979, Emeritus in 1994. He then joined the Inorganic Chemistry group of Professor Rudi van Eldik, as a Research Associate at the University of Erlangen-Nuremberg, until 1998, whereupon he became a Research Manager at Unilever Research, in the UK. Since 2002 he has served as Co-Editor for several Volumes of Advances in Inorganic Chemistry. He is a member of the Royal Society of Chemistry, the American Chemical Society, the American Society for Biochemistry and Molecular Biology, and The Arts Society, Rutland.

Rudi van Eldik received his PhD from Northwest University, South Africa, followed by a Habilitation at the Goethe University, Frankfurt/Main, Germany. He became a Full Professor of Inorganic Chemistry at the Private University of Witten/Herdecke in 1987, followed by a Chair for Inorganic and Analytical Chemistry at the Friedrich-Alexander University Erlangen-Nuremberg in 1994. After his retirement in 2010 he joined the Faculties of Chemistry at the Jagiellonian University in Krakow and the Nicolaus Copernicus University in Torun, Poland. He received honorary doctoral degrees from: Northwest University (South Africa), University of Kragujevac (Serbia), Jagiellonian University, Krakow (Poland), University of Pretoria (South Africa) and Ivanovo State University of Chemistry and Technology (Russia). He is the author of almost 1000 original papers and reviews, and Editor of Advances in Inorganic Chemistry (Academic Press) since vol. 54 of the series.

and Erlangen-Nuremberg, occurred in 1987 and 1994, respectively. Retirement appeared unthinkable and Rudi moved to a research Professorship in Chemistry at the Jagiellonian University in Krakow, Poland in 2010, and thence to a comparable position at Nicolaus Copernicus University in Torun, Poland a few years later. Currently he pursues research on several wide-ranging subjects in Torun, and enjoys research collaborations with colleagues in other research venues, as will be presented in the individual chapters that follow the Introduction.

Among the most remarkable aspects of his career is the incredible research versatility revealed by his publications record. This has now reached almost one thousand, with the vast majority of publications appearing in high-impact refereed journals. Naturally, this outstanding contribution to research has involved countless very capable research students, post-doctoral staff, habilitation candidates, research visitors and many other collaborative colleagues. The areas of expertise, invariably in pursuit of mechanistic enlightenment, include photochemistry of transition metal complexes and transition metal complex substitution mechanisms. In the latter category initially with Professor Kelm, Rudi became one, among others, at the forefront of applying high hydrostatic pressure to solution reactions to determine volume parameters that could be vital in support of mechanism diagnosis. Methods for monitoring reaction progress *in situ*, when under pressure, are rarely available from commercial instrument suppliers, necessitating design and construction of appropriate instrumentation for both conventional time range and very rapid reactions. Rudi and colleagues have published regularly regarding innovations and improvements in this context. Bioinorganic chemistry, including enzyme catalysis and model complexes became subject to the attention of sub-groups within his laboratories. The effect of solvent in kinetics studies is a longstanding variable in both organic and inorganic mechanistic chemistry. Rudi and his colleagues began an intensive pursuit of the consequence of studying the kinetics of inorganic reactions in ionic liquids. In parallel this involved an appraisal of the relative donor/acceptor properties of the component ions and their influence upon the reactants as well as the mechanism itself. Strict scrupulous purification of ionic liquids was one prominent finding; a requirement to prevent spurious results being obtained. There were successful mechanistic outcomes, and experimental results can be explained in terms of the physicochemical properties of the ionic liquid components and interactions with reactants and products.

Increasingly sophisticated computational methods for examining progress during reactions became available. Rudi, together with colleagues and expert collaborators have in the past twenty-five years applied these methods to a variety of reactions but particularly to solvent exchange at coordinated metal centers. The results can serve in support of solvent exchange experimentalists, particularly those using high pressure spectroscopy.

An examination of the publication record would indicate other research areas of interest to Rudi and his groups; high pressure electrochemistry, electron self-exchange reactions, environmental chemistry, applied analytical chemistry in the context of recycling potential of electronic devices and household products.

The co-authors of the publications are too numerous to list here, but can be accessed through- "Professor Rudi van Eldik – Publications List" from the internet.[1]

Recognition of the respect and status Rudi enjoyed within the Inorganic Chemistry community led to an invitation to serve as Series Editor of the Advances in Inorganic Chemistry series early in the new Millennium. Thirty Volumes have appeared since his appointment; these provide valuable reviews of specialized topics useful for research students and other investigators at early stages in their careers.

The boundless enthusiasm and curiosity in pursuit of research in the wide spectrum that is inorganic chemistry, Rudi extends to informing and entertaining the public, with chemistry demonstrations. This manifest itself into an annual event in a huge auditorium in Erlangen with several repeat performances. The program highlighted chemistry demonstrations, together with related themes of dialogue, and humor, by Rudi and participants from his research group, and directed at both adults and children. This event "The Magic Show" underlines the passion and indefatigability of Rudi that characterize his presence in the world of chemistry.

In 2009 he was awarded the Federal Cross of Merit ('Bundesverdienstkreuz') by the Federal President of Germany. This award was for his research work and for his development and participation in The Magic Show!

2. Nitrosylcobalamin – Latest Studies on Formation and Reactivity

At the beginning of the twenty-first century, it was reported that nitric oxide (NO) can react with the reduced form of Vitamin B12 (Cbl(II)) giving the nitrosylcobalamin (CblNO), the derivative of the cobalt(III) ion and coordinated NO^- ligand.[2] During the past 20 years since this discovery, numerous studies on the formation of nitrosylcobalamin have been reported. It was shown that CblNO can also be produced from the interaction of derivatives of Vitamin B12 with different HNO donors, e. g. Angeli's salt,[3] NONOates,[4] and as well can be formed as a product of the interaction between nitrocobalamin ($CblNO_2$) and ascorbic acid (Asc).[5,6] The purpose of this contribution is to summarize the latest studies concerning the reactions of CblNO formation.

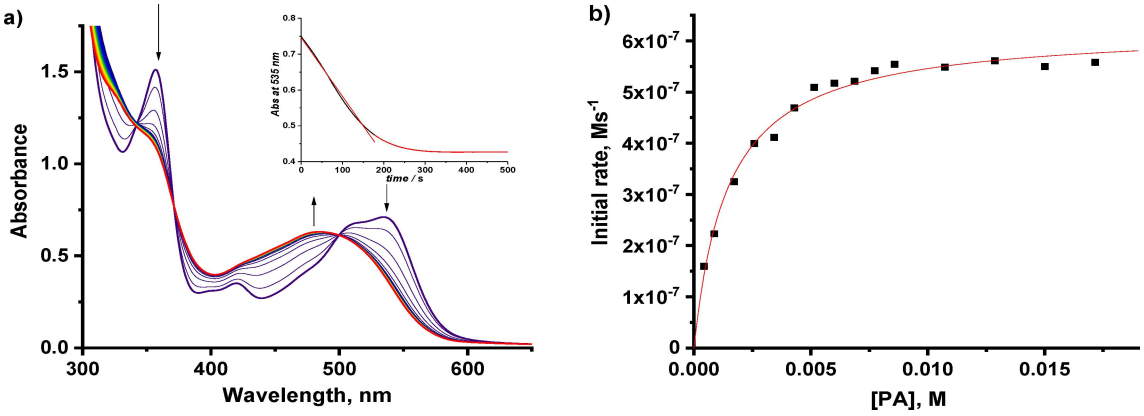

Figure 1. a) UV–Vis spectra recorded for the reaction of CblOH (8.5×10^{-5} M) with PA (0.013 M) at pH 10.2 under strictly anaerobic conditions (0.10 M carbonate buffer, 25.0 °C). Inset: Plot of absorbance at 535 nm versus time for the same reaction. b) Plot of the initial rate versus [PA] for the reaction of CblOH (8.5×10^{-5} M) with PA at pH 10.2 (0.1 M carbonate buffer, 25 °C, Ar atmosphere). a) and b) Copyrights: Reprinted with permission from: Inorganic Chemistry 2021, 60, 2964. Copyright 2003 American Chemical Society.

2.1 Reactions between CblOH/OH_2 and Piloty's Acid

Recently the formation of CblNO in the reaction between hydroxocobalamin/aquacobalamin (CblOH/OH_2) and HNO released from Piloty's acid (N-hydroxybenzenesulfonamide, PA) over the wide pH range (pH = 3.5—13.0) was described.[7] Piloty's acid which was first reported by Oscar Piloty at the end of the XIX century, is known as an HNO donor at basic pH.[8] Releasing of HNO requires PA deprotonation (pK_a(PA) = 9.26) which is followed by heterolytic cleavage of the S–N bond. Detailed mechanistic studies showed that at pH > 9 hydroxocobalamin (CblOH) reacts with HNO yielding CblNO (Figure 1a) and the rate-determining step at low concentrations of PA is the decomposition of PA giving HNO, which is followed by the reaction between HNO and CblOH. However, when the PA concentration is increased, the reaction between CblOH and HNO becomes the rate-determining step (Figure 1b). The stoichiometry of the reaction was studied at pH 10 and 12 and it was determined as 1 : 1 CblOH/PA. It was significant that the studies using a high excess of PA at pH 9.5-13.0 allowed the determination of the experimental value of the acidity constant (pK_a) for HNO (Figure 2). The value obtained for pK_a = 11.5 ± 0.4 was in good agreement with the literature data.[7]

Some surprising results are presented in the report, concerning the reaction of PA and $CblOH_2$ under neutral and mild acidic conditions. According to the literature under these conditions, Piloty's acid does not release HNO,[9] thus it was believed that the reaction between $CblOH_2$ and HNO cannot be observed. However, the reported studies unexpectedly proved that at neutral and mild acidic pH the formation of the nitrosylcobalamin (CblNO) is observed.[7] The kinetic and mechanistic studies suggest that under these conditions a two-

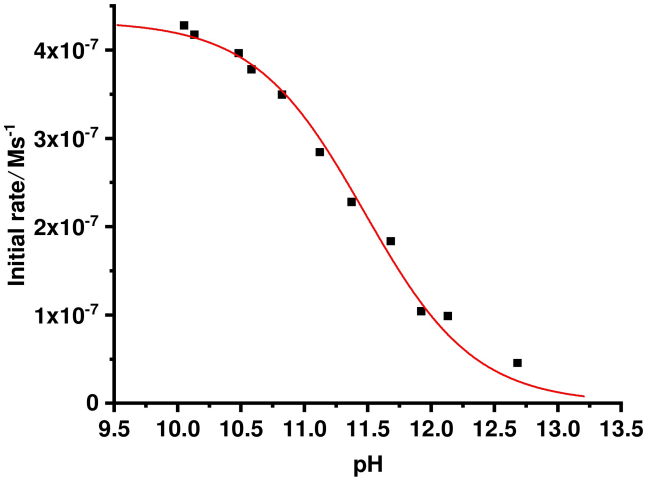

Figure 2. The plot of initial rate versus pH for the reaction between CblOH (8.5×10^{-5} M) and PA (0.013 M) under conditions where the rate–determining step is the reaction of HNO with CblOH to give CblNO. Reprinted with permission from: Inorganic Chemistry 2021, 60, 2964. Copyright 2003 American Chemical Society.

step reaction is observed. The first step provides direct interaction between $CblOH_2$ and PA, and the formation of a Cobalamin-PA intermediate. The second step is rapid deprotonation of the complex and S–N bond cleavage that gives CblNO and $PhSO_2^-$. Additional studies allowed the determination of the pK_a value for coordinated PA which is 5.5 (pK_a(CblPA) = 5.5 ± 0.1). Comparing the value obtained with the value of free PA indicates that the coordination of PA causes a 4 unit lowering of the pK_a value. All of the observed reactions in the system $CblOH_2$ – PA are summarized in Scheme 1.[7]

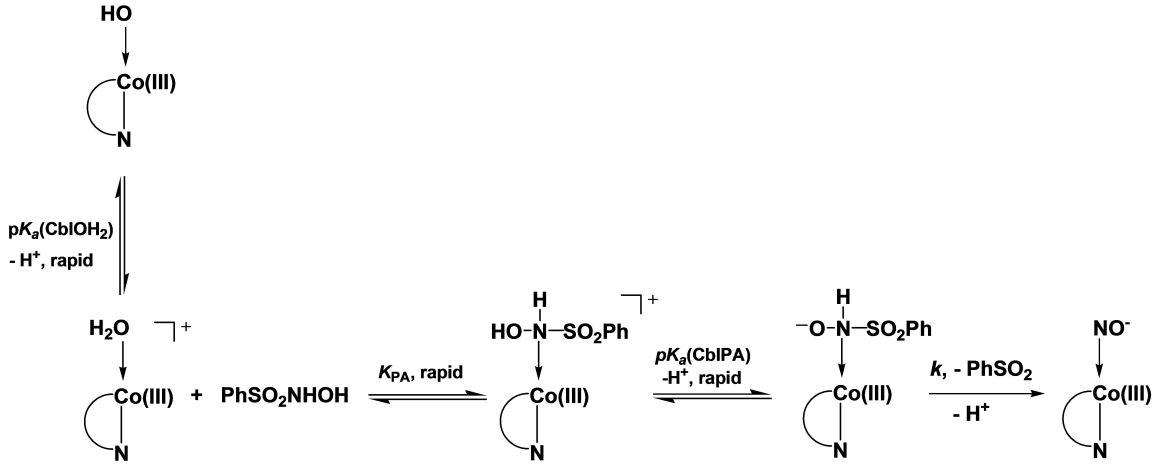

Scheme 1. Proposed scheme for the direct reaction between $CblOH_2$ and PA to form CblNO and $PhSO_2^-$. Reprinted with permission from: Inorganic Chemistry 2021, 60, 2964. Copyright 2003 American Chemical Society.

2.2 The reaction between $CblNO_2$ and Asc in the Presence of PM

Other later reports, focus on the reaction between nitrocobalamin ($CblNO_2$) and ascorbic acid.[5,6] It was also mentioned in our previous review,[10] that CblNO is formed in a multi-step chemical process in acidic pH (pH < 5). The reaction involves preliminary reduction of $CblNO_2$ to Cbl(II) and NO, which can subsequently react to yield CblNO (Scheme 2).[6] The studies did not provide any evidence for the reduction of coordinated nitrite. Recent studies on this system refer to the presence of particulate matter (PM) in the reaction solution and its influence on the kinetics and mechanism of CblNO formation. For this purpose, a series of experiments with the addition of the urban PM samples to the reaction mixture were conducted.[11–13] Thus, the authors discuss a very important topic – how air pollution and especially inorganic components affect the redox physiological/biological processes.[11–13] This aspect of the research involves both samples of the urban PM[11,12] as well as model compounds (nano metal oxides[11,13]).

In the case of urban dust samples, the role of reference material obtained from NIST (National Institute of Standard and Technology) (SRM 1648a), plasma-treated SRM (LAP), as well as samples collected in Kraków in both winter and summer seasons were studied.[11,12] First, it was demonstrated

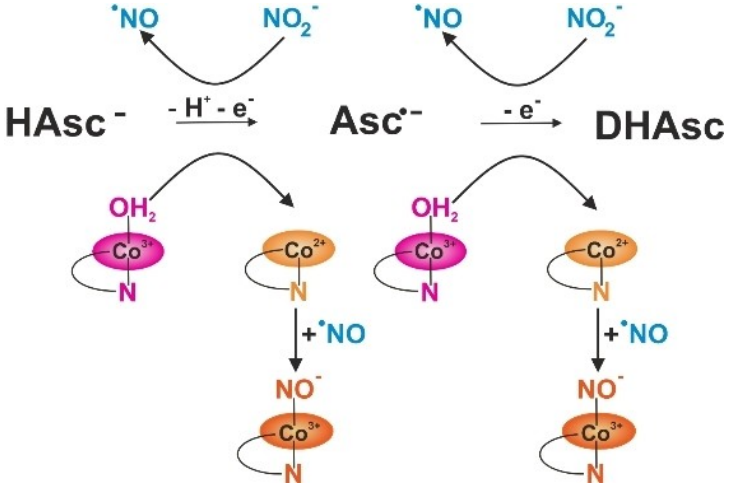

Scheme 2. Schematic presentation of the simultaneous reduction of nitrite and $CblOH_2$ by $HAsc^-$ to form CblNO in two subsequent reaction steps involving the ascorbate radical.[6,12] Copyrights: open access on license CC BY-NC-ND 4.0.

that addition of NIST PM extract accelerates CblNO formation. The observed rate constant for CblNO formation increases with increasing NIST PM concentration. However, when the organic component was removed from the NIST PM sample (plasma treated NIST- LAP), the opposite effect was observed.[11] The addition of Kraków dust samples caused similar effects as NIST PM samples. In both cases, winter and summer Kraków dusts, the presence of the material in the reaction mixture causes the acceleration of the reaction between $CblNO_2$ and Asc.[12] Interestingly for both winter and summer samples, the observed effect was similar. On the other hand, it was also demonstrated that the Kraków dust samples are characterized by similar amounts of the analyzed transition metal components as the NIST PM sample.[12] The results discussed can be explained by the report[11] in which the role of the content of Fe, Mn, Cu, and other transition metals, was studied. These studies demonstrated that while most of the redox-active metal oxide nanoparticles have an influence on the reaction between $CblNO_2$ and Asc, the non-redox-active metal oxide nanoparticles did not affect the reaction.[11] Especially interesting was the effect caused by nanoparticles of CuO; the addition of nanoparticles of CuO strongly accelerated the formation of CblNO. It was observed that the reaction was ca. 2–3 times faster than the reaction in the absence of nanomaterials (Figure 3a).[11,13] Modification of the surface of CuO nanoparticles by coating with polydopamine and the functionalization by o-(aminoethyl) polyethylene, maintained the catalytic activity of the nanomaterial towards reactions between $CblNO_2$ and Asc.[13] The observed changes in k_{obs} values caused by the presence of nanomaterials in the reaction solution are similar for both modified and unmodified nanoparticles of CuO (Figures 3a and 3b). On the other hand, it was demonstrated that modifications on nCuO surfaces provide improved stability of nCuO suspension in aqueous media compared to the unmodified nanoparticles and reduce the aggregation of the material.[13] The general conclusion that comes from the series of studies indicates that air pollution should be considered a significant factor in the pathology of these bioinorganic redox processes.

3. Reactions of NO with Microperoxidase-11 as a Heme-Protein Model

Evaluation of model complexes is a critical method in bioinorganic chemistry, which allows for better comprehension of the molecular mechanisms involved in metalloenzyme function. Such studies allow us to examine reaction kinetics in a less complex manner, without the interaction of the ligand with the protein matrix (while providing information concerning the specific function of the protein matrix in a given reaction) and assist in the identification of potential intermediates and side reaction products.[14,15] Model systems enable experiments to be conducted in strictly regulated conditions (very low temperatures, anaerobic or water-free reactions) which can facilitate the trapping of unstable intermediates and then investigation of molecular mechanisms occurring at the active site. Numerous previous reviews discuss in considerable detail, the molecular mechanisms of NO interaction with the heme center in model porphyrin systems.[16–18]

In nature, the covalent bonding of heme prosthetic groups is frequently observed in the cytochrome c family.[19] This bonding type involves the addition of sulfur from two cysteine residues across former vinyl groups in iron protoporphyrin IX. Microperoxidases (MPs), also known as heme-based mini-enzymes, are an instance of covalent bonding of the heme. These heme peptides are produced from c-type cytochromes by proteolytic digestion. They were named based on their

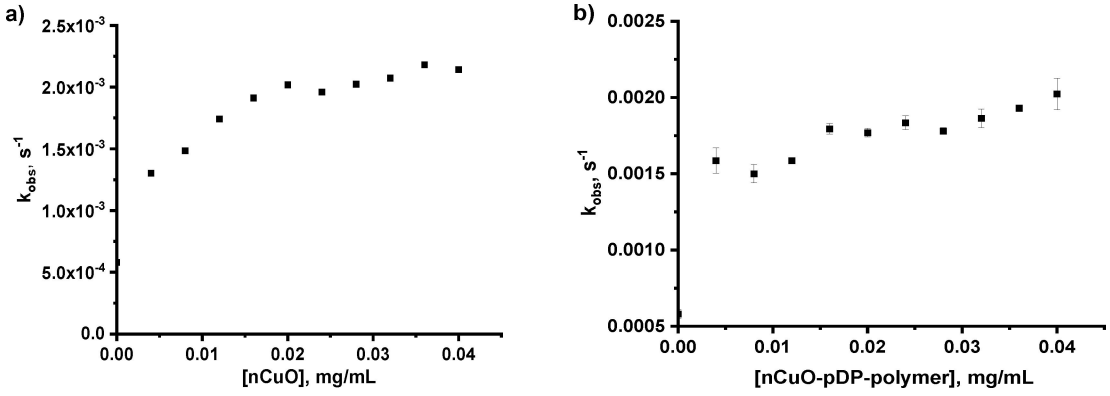

Figure 3. The plot of observed rate constant (k_{obs}) versus concentration of CuO nanoparticles **a)** and modified CuO nanoparticles **b)** for the reaction between $CblNO_2$ (8.6×10^{-5} M) and Asc (1.7×10^{-3} M) at pH 4.3 (25.0 °C, acetate buffer) during the formation of CblNO. The datum point at zero concentration is the reference value in the absence of any nanoparticles.[11,13] Copyrights: a) open access on license CC BY-NC-ND 4.0. b) Polyhedron, 2022, 223, 115942, Copyright 2023, with permission from Elsevier.

capacity to act as peroxidatic catalysts, which characteristic made them valuable as a model for examining the chemical reactions of native peroxidases and larger hemoproteins.[20] Thus far, a total of seven distinct MPs have been isolated, and they maintain the unchanging pattern of Cys-14-X-15-X-16-Cys-17-His-18 (using horse cytochrome c numbering) found in the parent protein (Figure 4). In this pattern, the Cys residues form a covalent bond with the porphyrin side-chains located at positions C3 and C8. The MPs are: MP-5 (amino acid residues 13–14/17-18), MP-6 (residues 14–19), MP-7 (residues 14–20), MP-8 (residues 14–21), MP-9 (residues 14–22), MP-10 (residues 13–22), and MP-11 (residues 11–21).[21–23]

Microperoxidases are recognized for retaining histidine 18 as the fifth ligand on the heme iron, which means that only one axial coordination site is occupied by a water molecule (at neutral pH), and this can be easily replaced by an external ligand (e.g., nitric oxide, carbon monoxide or cyanide).[24–26] In addition, they lack mechanisms for stabilizing their distal structures and kinetic barriers that are typically associated with protein structures.[27] As a consequence, microperoxidases are considered ideal model compounds for hemoproteins with at least one histidine axial ligand, such as hemoglobin and myoglobin, numerous cytochromes including b, c, and f, peroxidases, and cytochrome c oxidase. It should be noted that microperoxidases tend to aggregate at micromolar concentrations.[28,29] When appropriate precautions were not taken, the tendency of microperoxidases to aggregate in a concentration-dependent manner has resulted in unreliable data in studies involving heme-peptides. However, there have been significant efforts to address this issue, particularly in the case of ferric heme-peptides; various protocols have been developed to ensure that aggregation effects do not undermine future investigations. For example, one effective approach

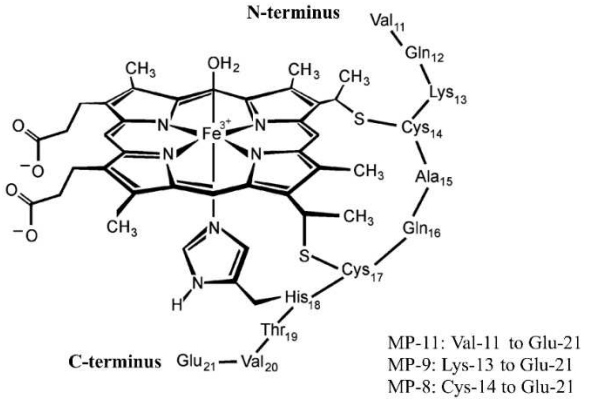

Figure 4. Molecular structure of MP-8, MP-9 and MP-11. Numbering of the amino acids is based on the sequence of cytochrome c from horse heart.[21]

involves the acetylation of the NH_2 groups of the peptide, which strongly inhibits aggregation.[21,29]

A noteworthy member of this group is MP-11, which is comprised of an undecapeptide attached to a heme c group. MP-11, along with MP-8 are the most studied while MP-11 is considered more convenient for investigation, as it is easier to prepare.[30] Microperoxidase-11 was the subject of extensive research in coordination and electrochemical studies (MPs exhibits peroxidase activity,[31] and the reduction potential depends on pH).[32] Microperoxidases can also be used potentially as biosensors and they can be successfully immobilized in solid matrices.[22,33,34]

Several studies utilized the MP-11 system with respect to the chemistry of nitric oxide. For example, Ascenzi *et al.* examined the NO_2^- mediated nitrosylation of ferrous-microperoxidase-11 and reductive nitrosylation of ferric-microperoxidase-11.[35,36] The authors studied factors responsible for the reactivity and the mechanism of reductive nitrosylation. It was found that this process occurs only above pH 8.2 for MP-11. Results suggest that the distal structure is a key factor for determination of the rate of NO association – the apparent rate constant for MP-11 nitrosylation has the highest value compared with the corresponding parameter for different heme-proteins, which indicates that MP-11 is a useful model for studying the Fe-heme reactivity. It was noteworthy that rate constants of NO binding did not show any clear trend with pH increase in the range of 7.0–9.2.[36] In addition, the authors stated that while the axial coordination of the metal center and the accessibility of ligands to the iron atom are major determinants of the reactivity of heme-based proteins and models, one also needs to consider other factors such as the reduction of the ligand binding energy barrier to the heme, and the limitation of degrees of freedom of the ligand conformation.

Microperoxidase-11 at alkaline pH exists in three acid-base forms: [(AcMP-11)Fe^{3+}(H_2O)(HisH)], [(AcMP-11)Fe^{3+}(OH)(HisH)] and [(AcMP-11)Fe^{3+}(OH)(His^-)].[30] Since according to the current paradigm the reactivity of the six-coordinate metal-hydroxo porphyrin complex should be limited by the dissociation of the OH^- ligand, the reported lack of pH-dependency of NO binding is surprising. Recently, a detailed kinetic study on NO binding to the acetylated form of microperoxidase-11 (AcMP-11), demonstrated a pH-dependent reactivity profile consistent with the existence of three acid-base related forms of microperoxidase in the pH range of 7.4–12.6 (Figure 5).[27]

However, the results show that a singly deprotonated form, (AcMP-11)Fe^{3+}(OH)(HisH), binds NO only about 10 times slower than (AcMP-11)Fe^{3+}(H_2O)(HisH) species, which is considered the labile form (owing to the dissociation of its H_2O axial ligand). Conversely, the doubly deprotonated form, (AcMP-11)Fe^{3+}(OH)(His^-), which previously was considered

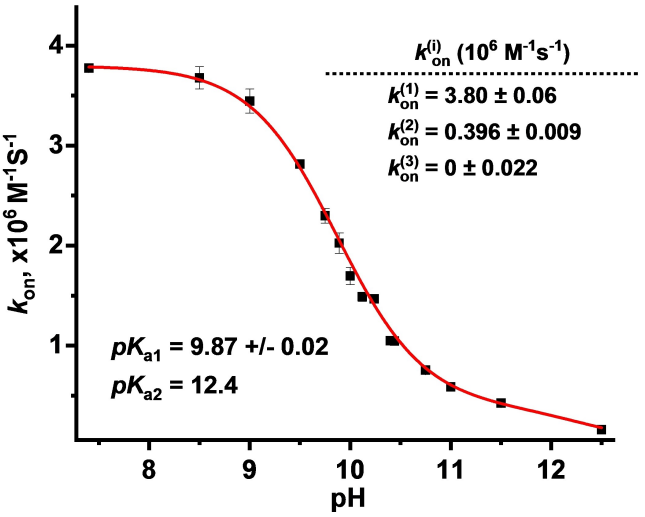

Figure 5. pH dependence of k_{on} for NO binding to AcMP-11 and the determined rate constants (T = 20 °C) for each of the three AcMP-11 acid-base forms.[27] Copyrights: open access on license CC BY 4.0.

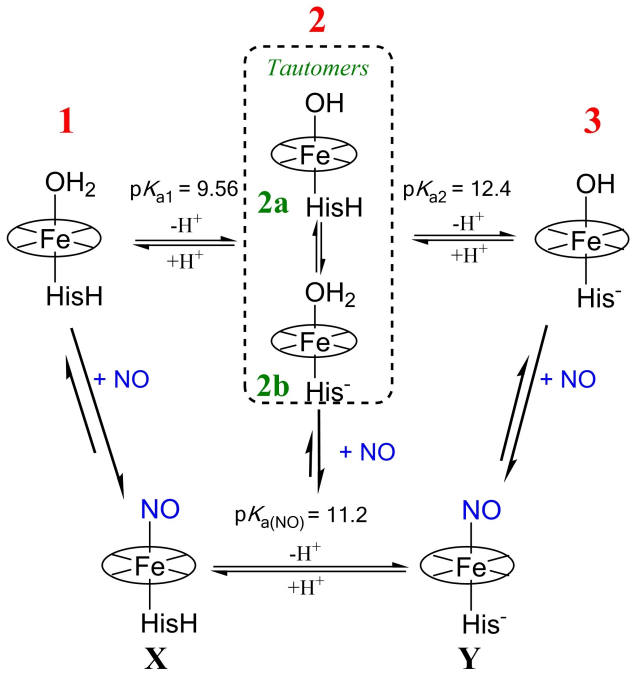

Scheme 3. Representation of pH–dependent reactivity pathways of AcMP-11 with NO.[27] Copyrights: open access on license CC BY 4.0.

as reactive due to the trans effect of His^-, was proven to be essentially inert. Quantum-chemical calculations provide an explanation for this peculiar reactivity indicating that (AcMP-11)Fe^{3+}(OH)(HisH) (previously identified as pure) coexists with its tautomeric form (AcMP-11)Fe^{3+}(H_2O)(His^-). The complex referred to possesses a labile Fe-OH_2 bond, which means that the H_2O ligand can be released to generate the five-coordinate complex, which is the intended site for NO binding (Scheme 3, species No 2). The proposed mechanism also provides an explanation for the inertness of the hydroxo complex with deprotonated histidine (Scheme 3, species No 3). Due to the lack of a proton source within it, the (AcMP-11)Fe^{3+}(OH)(His^-) does not undergo tautomerization to a reactive Fe-OH_2 species.

The findings presented in this study are at variance with the accepted view that the metal-hydroxo bond in a six-coordinate porphyrin complex is much less reactive in terms of ligand substitution when compared to the corresponding metal-aqua bond. In the heme center with two protic ligands; tautomerization equilibrium may tune the reactivity of the six-coordinate complex.

Recently, we utilized AcMP-11 to explore the mechanisms of S-nitrosothiols formation.[37] S-nitrosation is a selectively covalent modification of a thiol group of a cysteine to form S-nitrosothiol which has the general structure R–S–N=O. Apart from nitrosylation of the metal center of proteins (e.g. soluble guanylyl cyclase – the central NO receptor), S-nitrosation is one of the most important NO signaling pathways and plays a protective role against oxidative stress.[38–40] In proteins, it is an important post-translational modification affecting their activity. Low-molecular weight thiols play a critical role in extending nitric oxide life-time, its transport and S-nitrosation of protein sulfhydryl groups. Although formation of S-nitrosothiols has been extensively studied for many years, the molecular mechanism for RSNO formation in biological systems is still poorly understood.[41–44] One of the mechanisms proposed as being responsible for physiological S-nitrosothiols formation involves redox-active metal ions (Cu^{2+}, Fe^{3+}) and their complexes among which ferric-heme species may play particular roles. Ferric-heme complexes are perceived as electron acceptors that may fulfill redox requirements for the S-nitrosothiols generation.[45]

Research applying AcMP-11 as an electron acceptor showed that this heme-undecapeptide is able to transfer effectively NO to important biological thiols (RS), such as glutathione, cysteine, and N-acetylcysteine.[37] The extent of S-nitrosothiols produced depended on the concentration of both NO and thiol, with efficiency limited by the concentration of AcMP-11. Two potential reactivity pathways were evaluated, one involving the reaction of (AcMP-11)Fe^{3+}(RS) with NO, and the other involving the nucleophilic attack of a thiolate on (AcMP-11)Fe^{2+}(NO^+). Time-resolved spectroscopic studies showed that the double–step transformation process, completed accumulation of ferrous-nitrosyl microperoxidase-11, (AcMP-11)Fe^{2+}(NO), in both cases. The UV-Vis spectra characteristics of the captured intermediate products were identical in both reactivity scenarios, indicating the same coordination mode of RSNO to heme-iron, thus formation of

(AcMP-11)Fe^{2+}(N(O)SR). After conducting a thorough analysis of both the theoretical and kinetics data, it was found that nucleophilic attack of RS^- on (AcMP-11)Fe^{2+}(NO^+) was both kinetically and energetically more favorable, whereas formation of (AcMP-11)Fe^{2+}(N(O)SR) in direct attack of NO on coordinated thiolate in (AcMP-11)Fe^{3+}(SR) was excluded as a productive pathway. Scheme 4 presents the proposed mechanism of the RSNO formation with the assistance of microperoxidase-11 with the possible fate of the (AcMP-11)Fe^{2+}(N(O)SR) intermediate. Complete kinetic and thermodynamic characteristics of (AcMP-11)Fe^{2+}(N(O)SR) formation on the example of (AcMP-11)Fe^{2+}-N(O)AcCys) were presented, that point towards the feasibility of the proposed reaction mechanism to be biologically relevant. Additionally, it was revealed that the S–N bond in S-nitrosothiols is strengthened when the molecule coordinates with the heme-iron via nitrogen, rather than sulfur. Therefore, the preferred pathway for the generation of S-nitrosothiols with the assistance of heme-iron sites possessing proximal histidine ligand likely involves N-coordination of S-nitrosothiol in the axial position, while S-coordination promotes their decomposition.[37]

In another study, Đurović *et al.* applied NAcMP-11 to study the effects of standard particulate matter (SRM 1648a) on the activation of nitric oxide (NO) by iron heme proteins through kinetic analysis.[46] The impact of aqueous extracts from SRM1648a derived from PM suspensions and metal oxide nanoparticles (Fe_2O_3 and ZnO) on the binding of NO to AcMP-11 were investigated. The authors aimed to determine whether the constituents (soluble in water) extracted from an SRM 1648a sample could affect the reaction. However, no significant impact of the PM and nanoparticles on the kinetics of NO binding to AcMP-11 was observed. It is worth mentioning that research indicates the effect of particulate matter on the binding and release of dioxygen by deoxy-myoglobin, especially over extended periods of time.

4. Mixed-Valence Ru(II)/Ru(III) Ion-Pair Complexes

Mixed-valence complexes contain a metal present in more than one oxidation state.[47,48] Typical complexes from academic textbooks are the Creutz-Taube complexes,[49,50] Prussian Blue, molybdenum blue, and the oxygen-evolving center (OEC) of photosystem II. In these complexes, at least two metal centers are linked by a bridging ligand. A bridge can mediate intermetallic electron transfer from the reduced metal ion to the oxidized one. The bridged structure is typical for the majority of mixed-valence complexes.

Why are these compounds still being studied? Principally, they are very important in understanding many electron transfer processes, not only in the world of living organisms (e.g. metalloenzymes) but also in catalysis, the design of functional materials, and in molecular electronics. Mixed-valence complexes turn out to be excellent carriers for studying intramolecular electron transfer processes. Interestingly, the well-known Creutz-Taube complex $[\{(NH_3)_5Ru\}(\mu\text{-pz})\{Ru(NH_3)_5\}]^{5+}$, where pz = pyrazine, was used recently to control the excited state lifetime.[49]

In contrast, **mixed-valence ion-pairs**, in which metal centers in different oxidation states are not linked by a ligand, are not commonly reported. Among them are Co(II)/Co(III), Mn(II)/Mn(III), Fe(II)/Fe(III), and Pt(II)/Pt(IV) species, e.g. $Co_3^{III}O(O_2CPh)_3(pyCHNO)_3][Co_3^{II}(O_2CPh)_8]$,[51] $[Co^{II}_2(H_2L)_2(H_2O)_2][Co^{III}_2(H_2L)_2(H_2O)(m\text{-phth})]\cdot 8H_2O$ where H_2L^{2-} = 2-[(2-hydroxy-3-methoxybenzylidene)amino]-2-(hydroxymethyl)propane-1,3-diolato], m-phth = 1,3-benzenedicarboxylate,[52] $[Co^{II}(H_2O)_6][Co^{III}(C_{11}H_{14}N_2O_9)]_2$, $[Co^{II}(H_2O)_6][Co^{III}Br_2(C_2H_3N_2O_2)_2]_2$, $[Co^{II}(H_2O)_6][Co^{III}(C_9H_7NO_3)_2]_2\cdot 2H_2O$ and $[Co^{III}(en)_3]_2[Co^{II}L_2]_3\cdot 16H_2O$ where en = ethylenediamine, L = dipicolinate,[53–56] $[Fe^{II}(H_2O)_6][Fe^{III}(C_9H_7NO_3)_2]_2\cdot 2H_2O$[57] and $[Pt(NH_3)_4]^{2+}[PtCl_6]^{2-}$.[58] Some of them exhibit interesting chemical properties and/or activity. $[Mn^{II}(ntb)Cl][Mn^{III}$-

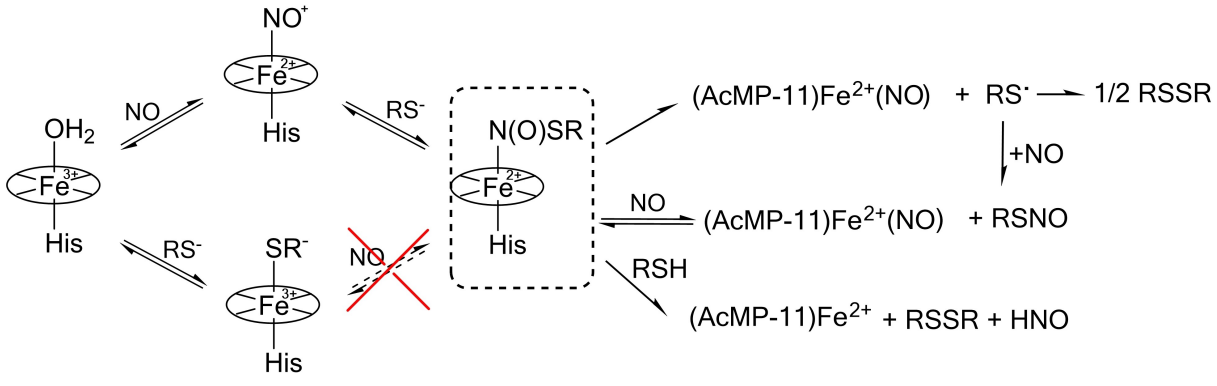

Scheme 4. Mechanism of AcMP-11 mediated S-nitrosothiols formation.[37] Copyrights: open access on license CC BY 4.0.

$(Br_4Cat)_2(H_2O)_2]\cdot 4H_2O$, where ntb = tris(2-benzimidazolylmethyl)amine, and Br_4CatH_2 = tetrabromocatechol, is a rare example of a complex ion-pair in the class of metal-dioxolane chemistry, shows strong catechol oxidase activity, attributed to the presence of both Mn(II) and Mn(III) centers.[59] An unprecedented mixed-valence cobalt(III)/cobalt(II) ion-pair complex is $[Co^{III}CO_3(bipy)_2]_2[Co^{II}(DCA)_2]\cdot 16H_2O$ where bipy = 2,2′-bipyridine, DCA = demethylcantharidate, exo-1,4-epoxy-cyclohexyl-2,3-dicarboxylate group, of the intriguing 3D supramolecular architecture. Its autooxidation product effectively captures atmospheric CO_2 to generate the corresponding carbonate complex.[60]

An interesting Fe(II)/Fe(III) mixed-valence ion-pair complex is $Fe^{II}(phen)_3][Fe^{III}(HATD)_2]_2\cdot 3DMA\cdot 3.5H_2O$, where phen = 1,10-phenanthroline, DMA = N,N-dimethylformamide and H_3ATD = azotetrazolyl-2,7-dihydroxynaphthalene.[61] It exhibits a high-temperature Fe(III) spin crossover, which mainly arises from π-stacking, hydrogen interactions, and Coulomb interactions between the $[Fe^{II}(phen)_3]^{2+}$ and $[Fe^{III}(HATD)_2]^-$ counterparts.

4.1 From Serendipity to Rational Design

Recently, we reported the synthesis of a Ru(II)/Ru(III) mixed-valence ion-pair complex.[62] The preparation of the complex was not intentional. It was formed during attempts to synthesize a Ru(III) complex with 2,2′-bipyridine (bipy) and picolinate (pic), an anion of pyridine-2-carboxylic acid. The surprise was all the greater since, to the best of our knowledge, there had been no previous reports in the literature on mixed-valence ion-pairs complexes of this metal, which stand in contrast to numerous mixed-valence Ru(II)-Ru(III) bridged binuclear complexes, e. g.[48,63–69] The serendipitous preparation of the first Ru(II)/Ru(III) mixed-valence ion-pair complex became an inspiration to synthesize more such compounds using 2,2':6',2"-terpyridine (terpy), 2,2′-bipyridine (bipy), and 1,10-phenanthroline (phen) as neutral chelating polypyridyl nucleophiles. A series of three ion-pair complexes of different cationic and common anionic counterparts was isolated: $[Ru^{II}(bipy)_2(pic)]^+[cis\text{-}Ru^{III}Cl_2(pic)_2]^-$ (**1**), $[Ru^{II}(terpy)(bipy)Cl]^+[cis\text{-}Ru^{III}Cl_2(pic)_2]^-\cdot(CH_3)_2CO\cdot H_2O$, (**2**), and $[Ru^{II}(terpy)(phen)Cl]^+[cis\text{-}Ru^{III}Cl_2(pic)_2]^-\cdot 2H_2O$, (**3**).[62,70,71] The compounds were identified, and their structures in the solid state were determined by applying single-crystal X-ray diffraction and FT-IR spectroscopy. Ligand environments and oxidation states of the ruthenium centers were characterized using EPR spectroscopy and from measurements from performing magnetic measurements. The identities of the species in aqueous solutions were established in UV-Vis absorption spectroscopic and mass spectrometry studies. The latter techniques, along with SEM/EDX and X-ray powder diffraction, confirmed the purity and homogeneity of all the salts obtained. The redox behavior of the ion-pair complexes was examined with the CV method. The structures of (**1**)–(**3**) along with the structure of $[H(Hpic)_2][cis\text{-}RuCl_2(pic)_2]\cdot 2H_2O$ (**4**), which was the source of the anionic part of the ion-pair complexes, $cis\text{-}Ru^{III}Cl_2(pic)_2]^-$, are presented in Figure 6.

The ruthenium(III) ion in complex (**4**) is surrounded by two chloride anions, positioned *cis* to each other, two nitrogen atoms in *trans* positions, and two oxygen atoms in *cis* positions from the coordinated picolinato ligands, Figure 6. The complex adopts the structure of a slightly distorted octahedron. The Ru–N and Ru–O bonds are much shorter (2.0516(19) and 2.0242(16) Å) than the Ru–Cl bond length (2.3422(6) Å).[71] The structures of anionic counterparts of the complex ion-pairs are very similar to that of (**4**) with Ru–N and Ru–O bonds shorter than Ru–Cl bonds.[62,70]

The IR spectra of the solid ion-pair complexes present the characteristic absorptions of both the coordinated picolinate anion, bipyridine, terpyridine, phenanthroline, and metal-ligand bonds. The characteristic sharp and strong or medium bands at 1464, 1282, 1238, 1047, 861, 766, 690, and 464 cm^{-1} are consistent with literature data for *mer*-$[Ru(pic)_3]$.[72] Many absorption bands are also seen in the far infrared region. They arise from metal-ligand interactions (Ru–N, Ru–O, and Ru–Cl).[16,24–26] Bands in the range of 325–330 cm^{-1} were assigned to Ru–N(pyridine) stretching vibrations. Bands around 425 and 465 cm^{-1} were assigned to ν(Ru–N) and ν(Ru–Cl), respectively. The far-IR spectra of all complexes (**1-4**) exhibit bands at about 282 and 245 cm^{-1} associated with Ru–Cl symmetric and asymmetric stretching vibrations, respectively.[62,70–72]

Spectacular results were obtained from EPR studies of compounds. As expected, the solid state EPR spectrum of (**4**), the anionic counterparts of **(1)–(3)**, (Figure 7) exhibit two distinct resonances characteristic of the $S = {}^1/_2$ spin system, with $g_\perp = 2.51$ and $g_{||} = 1.70$. The axial nature of the spectrum indicates the asymmetry of the electronic environment around ruthenium(III), in line with its distorted octahedral ligand environment observed in the crystal structure. This observation is consistent with an effective magnetic moment of 2.04 B.M., determined for **(4)**.[71] The value is typical of a one unpaired electron system and consistent with low-spin d^5 ruthenium(III), where the orbital degenerated $^2T_{2g}$ (O_h) ground state is split due to low symmetry ligand field effects and spin-orbit coupling. Since **(1)–(3)** are composed of anions of **(4)** and diamagnetic d^6 Ru(II) cations, silent in terms of EPR spectroscopy, one would predict magnetic and EPR features of the ion-pair complexes similar to those observed for **(4)**. Indeed, effective magnetic moments of 2.05, 2.08 and 2.13 B.M. (measured at room temperature) were established for **(1)**, **(2)**, and **(3)**, respectively.[62,70]

The EPR data collected for **(2)** and **(3)** are typical for low-spin d^5 species as well. The rhombic signals with the principal

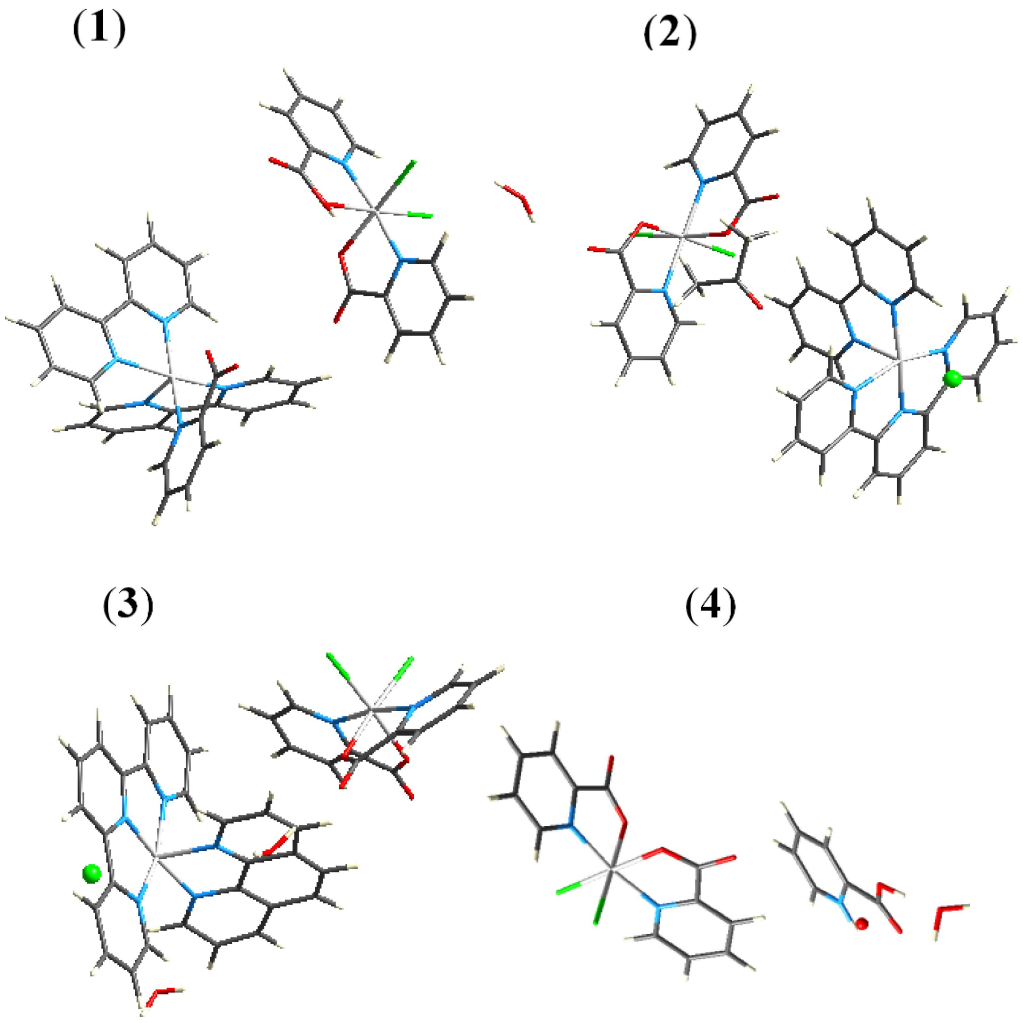

Figure 6. Asymmetric part of the mixed-valence ion-pairs (**1**–**3**) and $[H(Hpic)_2][cis\text{-}RuCl_2(pic)_2]\cdot 2H_2O$ (**4**).

g components are similar to those of **(4)** and in line with the crystallographically observed deformed octahedral structural units $[cis\text{-}Ru^{III}Cl_2(pic)_2]^-$.[62,70,71] Summing up, as predicted, the EPR spectra of (**2**), (**3**), and **(4)** were characteristic of species in a doublet state ($S=^1/_2$ spin system).

Surprisingly, the EPR spectrum of (**1**) is not typical for a species in a singlet state ($S=^1/_2$ spin system).[62,70] On one hand, its middle- and high-field part of rhombic nature (which indeed is in line with the distorted octahedral geometry of the anionic Ru(III) counterpart) exhibits the distinct resonance that could be assigned to the $S=^1/_2$ spin system. On the other hand, at the low-field range, the spectrum shows two additional lower-intensity signals with $g=5.2$ and 3.1, which cannot be accounted for in terms of an $S=^1/_2$ system. Interestingly, the EPR spectrum of a frozen solution of (**1**) at 77 K shows a typical rhombic nature according to $S=^1/_2$ spin, Figure 8.[62] Detailed solid-state low temperature (30 K) high-field EPR studies show that (**1**) has an $S=1$ system characteristic, which could originate from interactions between its Ru(III) anionic counterparts. This, in turn, would result in discrete Ru(III)-Ru(III) dimer coupling and a total $S=1$.[62] Indeed, thorough analysis of the crystallographic data revealed intermolecular π···π interactions between 6-membered rings of two picolinate ligands of $[cis\text{-}Ru^{III}Cl_2(pic)_2]^-$ units in all the ion-pair complexes, Figure 9.[62,70] As shown in Figure 9, one, four, and two types of the π···π interactions between Ru(III) moieties were found for (**1**), (**2**), and (**3**), respectively. However, the distances between two interacting picolinate anions of $[cis\text{-}Ru^{III}Cl_2(pic)_2]^-$ units in (**1**) are shorter than in (**2**) or (**3**), Figure 9. Therefore, the π···π interactions are stronger in (**1**) than in (**2**) which, in turn, are stronger than in (**3**). Thus, the Ru(III)-Ru(III) dimer coupling is much more efficient in (**1**) than in (**2**) or (**3**). These crystallographic findings account for an unexpected triplet state, $S=1$, of

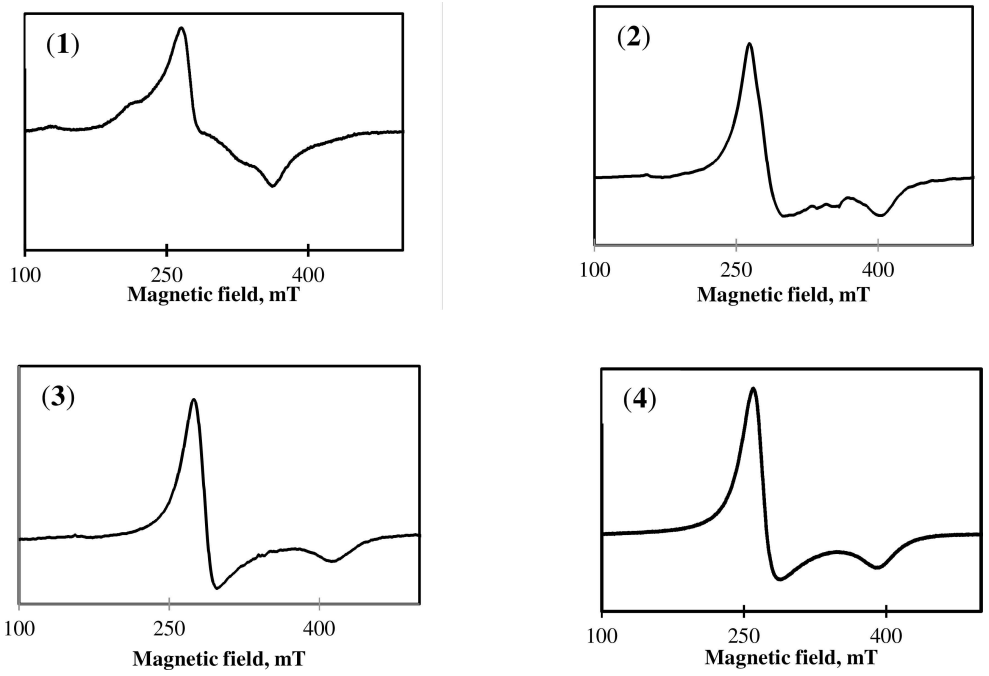

Figure 7. EPR spectra of powdered **(1)** and **(4)**, and **(2)** and **(3)** complexes, recorded at 9.3242 GHz at room temperature and 9.6 GHz at 77 K, respectively.[62,70,71]

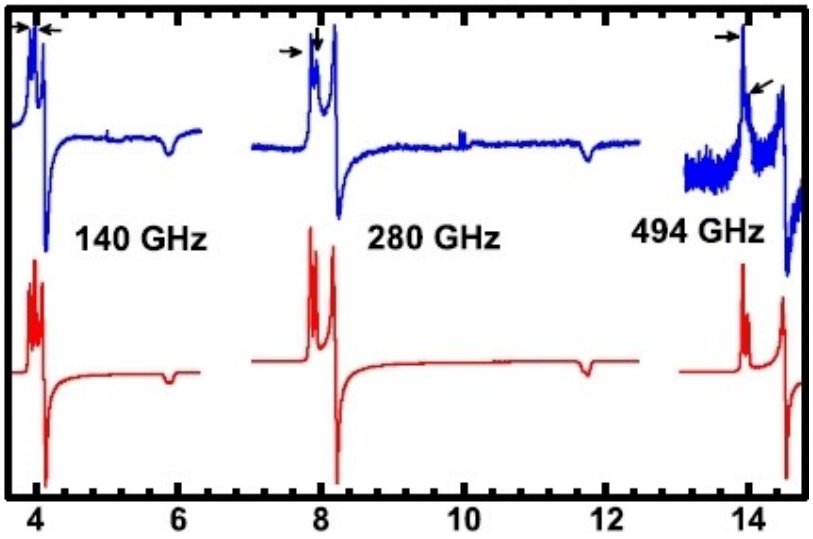

Figure 8. Solid-state (– experimental (blue) and – simulated (red)) – EPR spectra of $[Ru^{II}(bipy)_2(pic)]^+[cis\text{-}Ru^{III}Cl_2(pic)_2]^-$ (**1**) recorded at: (A) 140 GHz, (B) 280 GHz, and (C) 494 GHz at 30 K.

$[Ru^{II}(bipy)_2(pic)]^+[cis\text{-}Ru^{III}Cl_2(pic)_2]^-$ (**1**), manifested in its unique EPR properties.

The mixed-valence ion-pair complexes described above are of great interest not only because of the EPR results obtained but also because of the potential application of these compounds. Ion-pairs of the ruthenium constituents in two different oxidation states might have interesting material properties (redox catalysts) as well as therapeutic properties (antineoplastic drugs). Another challenge would also be to consider using them in the redox biology of cells.

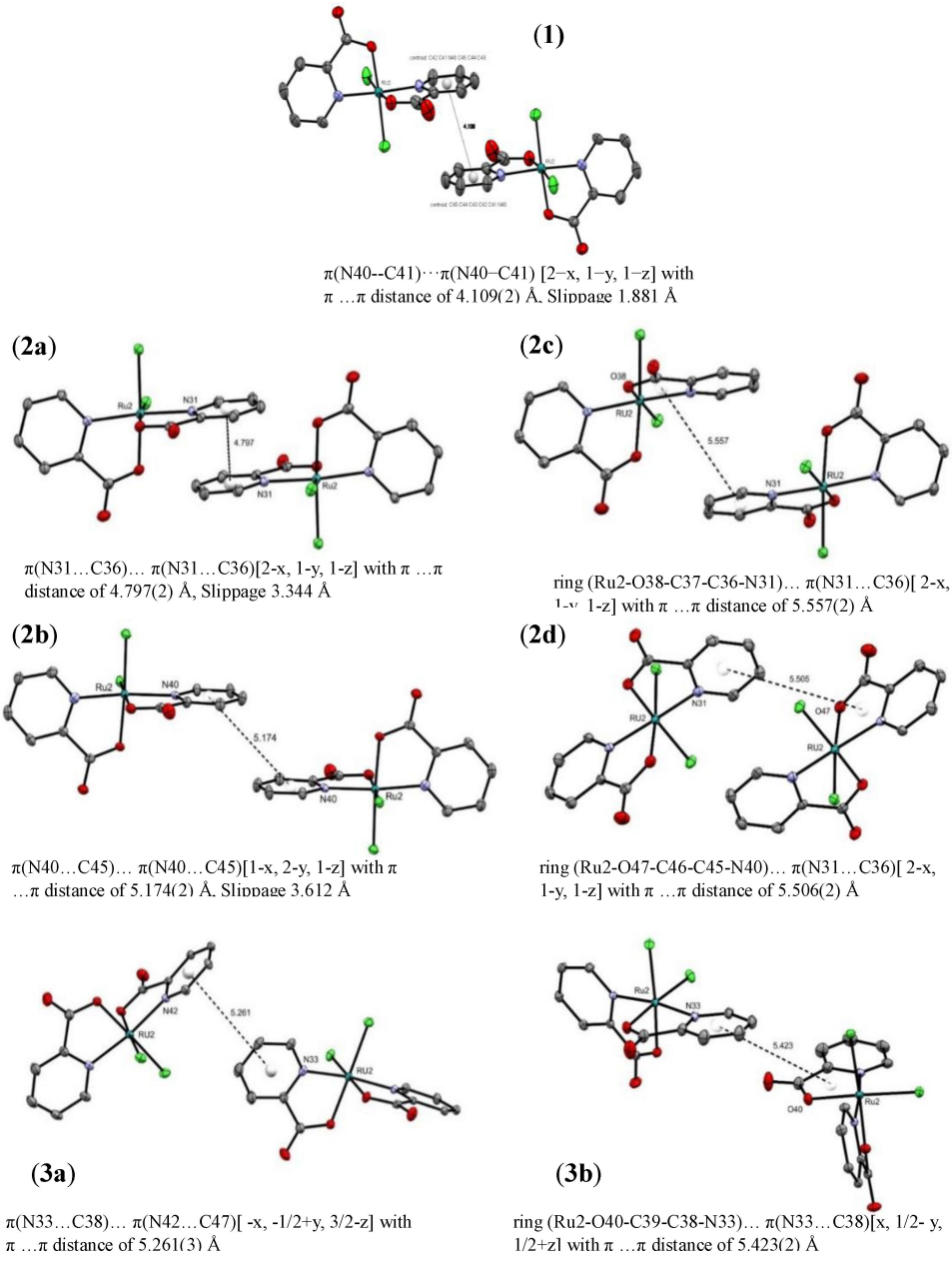

Figure 9. π···π interactions between *cis*-$[Ru^{III}Cl_2(pic)_2]^-$ anions in the **Ru^{III}…Ru^{III}** dimer in $[Ru^{II}(bipy)_2(pic)]^+[cis\text{-}Ru^{III}Cl_2(pic)_2]^-$ (**1**), $[Ru^{II}(bipy)(terpy)Cl]^+[cis\text{-}Ru^{III}Cl_2(pic)_2]^-$ (**2a–d**), and $[Ru^{II}(terpy)(phen)Cl]^+[cis\text{-}Ru^{III}Cl_2(pic)_2]^-$ (**3a–b**) ion-pair complexes. [62,70]

5. Reactivity of Ru(III/II)(edta) Complexes: Kinetic Lability and Redox Ability

The factors that primarily determine the reactivity of these metal complexes in solution are their lability towards binding substrate molecules and their redox ability of the metal centers to activate electron transfer reactions effectively.

In the $[Ru^{III}(Hedta)(H_2O)]$ complex, the 'Hedta^{3-}' ligand forms a 1:1 complex with ruthenium, and acts as a pentadentate coordinating ligand while the sixth coordination site of the ruthenium center is occupied by a water molecule. However, with an increase in pH of the solution, deprotonation of the dangling carboxylic acid group and the coordinated water molecule occurs successively as shown in (Scheme 5).[73,74]

Coordination of the penta-coordinating edta ligand highly labilizes both the Ru(III) and Ru(II) complexes towards an aqua-substitution reaction as compared to their pentaammine

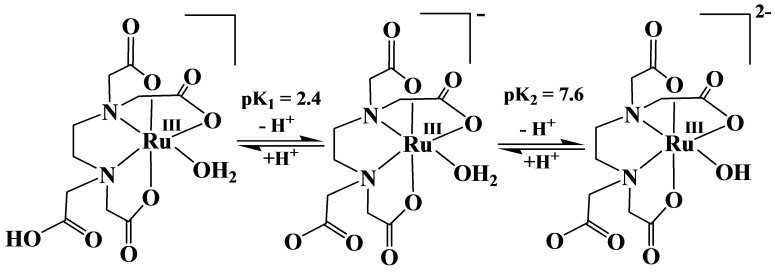

Scheme 5. Acid dissociation equilibria of the $[Ru^{III}(Hedta)(H_2O)]$ complex in aqueous medium.

analogs.[75,76] However, in contrast to the pentaammine complex of ruthenium(II), the reactivity of the edta complex of ruthenium(II) towards aqua-substitution is lower than that of its Ru(III)-analog. As a consequence of the kinetic lability of the Ru(III) analog towards the aqua substitution reaction, it affords a facile and straightforward method of binding substrate molecules, especially with small molecules. Apart from this kinetic lability, the results of electrochemical studies of a range of mononuclear and binuclear complexes of Ru(edta), a topic which has been reviewed recently,[77] signifies their potential to act as redox mediators or catalysts. In this article, we have summarized our current understanding of the mechanistic aspects of Ru(edta) catalyzed redox reactions in resemblance to metalloenzymes.[78]

5.1 Lability of $[Ru^{III/II}(Hedta)(H_2O)]^{0/-}$ Towards Aqua-Substitution Reactions

During the late nineteen seventies to the late-nineties, the $[Ru^{III}(edta)(H_2O]^-$ complex was subjected to kinetic and mechanistic studies pertaining to aqua-substitution reaction with various substituting molecules (L).[76,79–87] Binding to edta labilizes both the Ru(III) and Ru(II) metal centers towards aqua-substitution reactions, with the extent of the labilization being much greater for Ru(III). The rate of aqua-substitution reactions of $Ru^{III}(edta)$ complexes outlined in (Eqs 1–3) is highly pH dependent because of the substitution lability of various $[Ru^{III}(Hedta)(H_2O)]$, $[Ru^{III}(edta)(H_2O)]^-$ and $[Ru^{III}(edta)(OH)]^{2-}$ species in equilibria (Scheme 5). The maximum reactivity of the substitution reaction is observed in the pH range 4–6, and in this pH range the metal complex exists predominantly as $[Ru^{III}(edta)(H_2O)]^-$.[74] In contrast to other ruthenium(Ill) complexes containing N and O donor atoms (which undergo aqua-substitution reaction at a very slow rate),[75,76] the unusual lability of the coordinated water molecule in $[Ru^{III}(edta)(H_2O)]^-$ towards substitution reactions is explicable in terms of an internal associative interchange (I_a) pathway via its own pendant uncoordinated -COO group wherein the *syn* lone pair of electrons of the carbonyl oxygen atom labilizes the coordinated water molecule.[74]

$$[Ru^{III}(Hedta)(H_2O)] + L \xrightarrow{k_1} [Ru^{III}(Hedta)(L)] + H_2O \quad (1)$$

$$[Ru^{III}(edta)(H_2O)]^- + L \xrightarrow{k_2} [Ru^{III}(edta)(L)]^- + H_2O \quad (2)$$

$$[Ru^{III}(edta)(OH)]^{2-} + L \xrightarrow{k_3} [Ru^{III}(edta)(L)]^- + OH^- \quad (3)$$

Noteworthy here is that the rate of aqua-substitution is much greater for Ru(III) than for Ru(II) in contrast to the order of reactivity of other ruthenium(III/II) complexes. For example, the substitution rate constant for the reaction of $[Ru^{III}(edta)(H_2O)]^-$ with isonicotinamide ($k_2 = 8300\ M^{-1}s^{-1}$ at 25 °C) is much higher than that observed for the reaction of $[Ru^{II}(edta)(H_2O)]^{2-}$ with isonicotinamide ($25\ M^{-1}s^{-1}$ at 25 °C).[76] On the other hand while aqua-substitution of $[Ru^{III}(NH_3)_5(H_2O)]^{3+}$ with pyrazine/isonicotinamide is considerably slow ($\sim 10^{-6}\ M^{-1}s^{-1}$ at 25 °C), the ruthenium(II)-analog undergoes aqua-substitution with a much higher rate constant ($0.1\ s^{-1}$ at 25 °C).[75] Labilization of $[Ru^{II}(edta)(H_2O)]^{2-}$ may be ascribed to an electrostatic reduction (lowered the effective charge on the metal center) of the barrier to a dissociative substitution process. It is significant that unlike the Ru(III)-analog, aqua-substitution of $[Ru^{II}(edta)(H_2O)]^{2-}$ shows no pH dependence (in acid solution) and no large sensitivity to the nature of the incoming ligand (L). It is important to mention that the results of the kinetic studies along with the mechanistic details pertaining to the reaction of the $[Ru^{III}(edta)(H_2O)]^-$ complex with DNA and DNA constituents, cellular thiols, and nitric oxide (NO) highlighting the prospect of Ru(edta) complexes as metallo-pharmaceuticals were systematically reviewed earlier.[88] However, kinetic data pertinent to the substitution of the $[Ru^{III}(edta)(H_2O)]^-$ complex by various nucleophiles reported so far, are summarized in Table 1. The data in Table 1 may be of value in rationalizing the nucleophilicity of various substrate

Table 1. Rate constants and activation parameters for the reaction of $[Ru^{III}(edta)(H_2O)]^- + L \rightarrow [Ru^{III}(edta)(L)]^- + H_2O$. Part of the data in Table 1 reproduced from Coord. Chem. Rev. 1998, 168, 273 with permission from Elsevier.

L	k_2 ($M^{-1}s^{-1}$)[a]	$\Delta H^{\neq}$ (kJ mol^{-1})	$\Delta S^{\neq}$ ($Jmol^{-1}K^{-1}$)	$\Delta V^{\neq}$ (cm^3 mol^{-1})	Ref.
Pyrazine	20,000	24	−84		[76]
Pyridine	6300				[76]
Isonicotinamide	8300	28	−80		[76]
Imidazole	1860				[76]
Acetonitrile	30	35	−101		[76]
Azide	1885	25	−99	−9.0	[83]
Thocyanate	270	37	−75	−9.5	[83]
Thiosulfate	2.9				[80]
Thiourea	2970	22	−108	−6.8	[83]
Dimethylthiourea	1450	25	−107	−8.8.	[83]
Tetramethylthiourea	154	30	−107	−12.2	[83]
Dimethylsulfoxide	11	33	−126		[89]
Cyanide	1.1				[90]
Chloride	8.7				[91]
N-hydroxyurea	6.8	52	−53	−16	[92]
L-Arginine	10.4	39	−128		[93]
Adenine	8840				[94]
Adenosine	8901				[94]
Adenosinmonophosphate	2905	33	−67		[94]
Adenosindiphosphate	1786[b]	37	−55		[94]
Adenosintriphosphate	1068	38	−59		[94]
Guanosinmonophosphate	29	35	−100		[95]
Inosinmonophosphate	38	34	−100		[95]
Cytosine	1.8				[86]
Cytidine	1.5				[86]
Cysteine	170	40	−69		[87]
N-acetylcysteine	240	39	−74		[87]
Penicillamine	16	46	−58		[87]
Glutathione	260	68	−77		[87]
Glycine	24	57	−31	−3.3	[96]
Captopril	246				[97]
Nitric oxide (NO)	1.4×10^7 [c]				[98]
Nitrite	271	41	−98		[99]
Bicarbonate	82				[100]
Hydrazine	0.576[d]				[101]

[a] Temp. = 25 °C, pH = 5.0. [b] 20 °C, pH 4.6 [c] Temp = 7.3 °C, pH = 6.5 [d] Temp = 25 °C, pH < 4.5

molecules towards binding to $[Ru^{III}(edta)(H_2O)]^-$ through the aqua-substitution reaction.

It may be noted that because of the associative mode of activation (I_a), the rate constant values (Table 1) for aqua-substitution of $[Ru^{III}(edta)(H_2O)]^-$ are sensitive to the nature of the entering ligand (L). The identity of the substituting ligand (L) is decisive in determining the substitution rate, and the extent of bond-making in the transition state. For example, the aqua-substitution rate of $[Ru^{III}(edta)(H_2O)]^-$ with the neutral ligand, thiourea decreases significantly with the increase in steric crowding on thiourea; $k_2^{TU} > k_2^{DMTU} > k_2^{TMTU}$ (where TU = thiourea, DMTU = dimethylthiourea and TMTU = tetramethylthiourea).[83] The activation parameters (Table 1) for the aqua-substitution reactions featuring small values of $\Delta H^{\neq}$, along with the large negative values of $\Delta S^{\neq}$ (Table 1) are characteristic for associatively activated processes. However, values of $\Delta V^{\neq}$ offer further insight into the transition state of the reaction. For example, $\Delta V^{\neq}$ values become more negative in the succession for L = TU, DMTU, and TMTU (Table 1) signifying the increased overlap of the van der Waals radii in the transition state with increasing partial molar volume of the entering group.[83]

5.2 Electrochemistry of Ru^{III}(edta) Complexes

The electrochemical behavior of the $[Ru^{III}(Hedta)(H_2O)]$ complex is schematically shown in Scheme 6. The one-electron reduction of $[Ru^{III}(Hedta)(H_2O)]$ to $[Ru^{II}(Hedta)(H_2O)]^-$ was found to be reversible in the pH range 3–5 and the $E_{1/2}$ values corresponding to the Ru^{III}/Ru^{II} redox couple became more

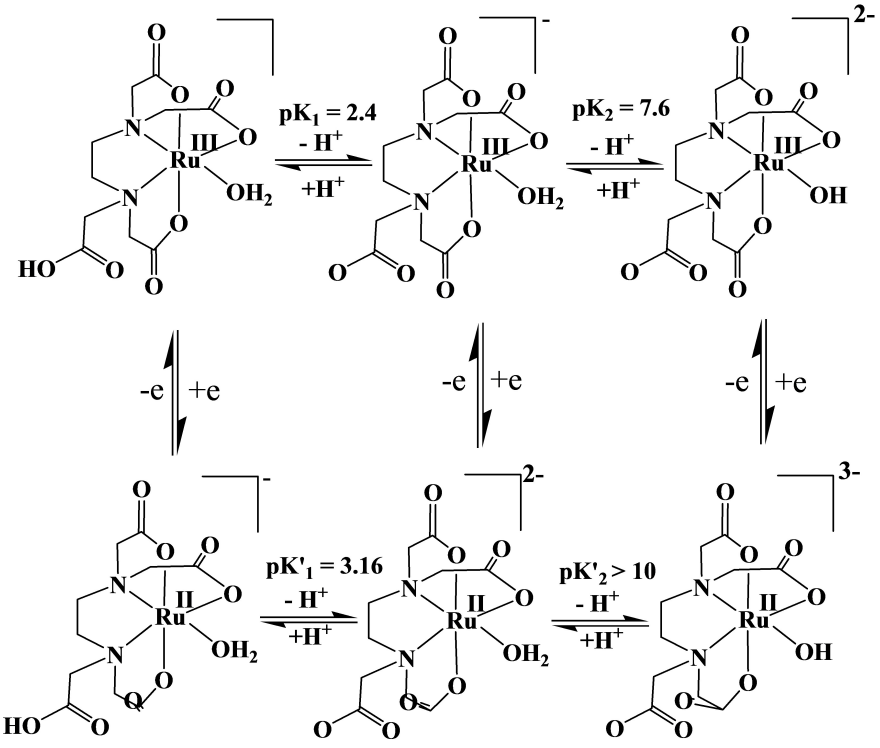

Scheme 6. Electrode reactions and proton dissociation equilibria of $[Ru^{III/II}(Hedta)(H_2O)]^{0/-}$ complexes. Reproduced from Chem. Rev. 2021, 436, 213773 with permission from Elsevier.

negative with increasing pH, and tended to reach a limiting value at a pH higher than 5.0.

The pH dependency of the $E_{1/2}$ values corresponding to the Ru^{III}/Ru^{II} redox couple may be explained in terms of the proton dissociation of the uncoordinated –COOH group as shown in Scheme 6. At higher pH (>6) lack of reversibility was noticed because of the considerable difference in the proton-dissociation equilibrium (Scheme 6) values of $[Ru^{III}(edta)(H_2O)]^-$ ($pK_{a2}=7.6$) and $[Ru^{II}(edta)(H_2O)]^{2-}$ ($pK'_{a2}>10$) complexes.[102] It is noteworthy that the reversibility of the reactions at the electrode diminished in the following order: HDME (hanging drop mercury electrode) > PBE (platinum button electrode) > PGE (pyrolytic graphite electrode).[76]

The $[Ru^{III}(edta)(H_2O)]^-$ complex readily reacts with different incoming ligands, L (L = monodentate ligands) to form $[Ru^{III}(edta)(L)]^-$ complexes (charge on the substituting monodentate ligands, L is omitted for the sake of convenience) through a straightforward water displacement reaction. We have recently reviewed[77] the electrochemical properties of several $[Ru^{III}(edta)(L)]^-$ complexes mostly exhibiting reversible metal-based electron transfer (Eq. 4). The values of the formal potential reported for the $[Ru^{III}(edta)L]^-/[Ru^{II}(edta)L]^{2-}$ couple in $Ru^{III}(edta)(L)]^-$ complexes are listed in Table 2. The $E_{1/2}$ values (Table 2) suggest how the nature of the ligands L influences the redox chemistry of the $[Ru^{III}(edta)(L)]^-$ complexes.

$$[Ru^{III}(edta)(L)]^- \underset{-e}{\overset{+e}{\rightleftharpoons}} [Ru^{II}(edta)(L)]^{2-} \quad (4)$$

However, a ligand-based (L = NO) electron transfer process (5 and 6) was observed[103] in the $[Ru^{III}(Hedta)(NO)]$ complex.

$$[Ru^{III}(Hedta)(NO)] \longleftrightarrow [Ru^{II}(Hedta)(NO^+)] \quad (5)$$

$$[Ru^{II}(Hedta)(NO^+)] \xrightarrow[-0.07V\ (vs.SHE)]{+e,\ pH=1.2} [Ru^{II}(Hedta)(NO^0)]^- \quad (6)$$

It should be noted that the $[Ru^{III}(Hedta)(NO^+)]^+$ complex (prepared by reacting $[Ru^{III}(Hedta)(H_2O)]$ with $NOBH_4$) undergoes a metal-based redox reaction at the electrode exhibiting an $E_{1/2}$ value (estimated by cyclic voltammetry) of −0.07 V (vs. SHE)[104] for the Ru^{III}/Ru^{II} redox couple.

In our recent review,[77] the intriguing electrochemical properties of Ru(edta) complexes are thoroughly evaluated. A wide range of metal-centered redox potentials observed for $[Ru^{III}(edta)L]$ complexes (Table 2) could contribute to an

Table 2. Formal potentials ($E_{1/2}$) for Ru^{III}/Ru^{II} couple in $[Ru^{III}(edta)(L)]^-$. Potentials are converted into SHE values for that were reported with different reference electrodes. Reproduced from Coord. Chem. Rev. 2021, 436, 213773 with permission from Elsevier.

Mono-dentate ligand (L)	$E_{1/2}$ (V vs. SHE)	Ref.
Uracil	−0.23	[105]
Nitric oxide	−0.11	[103]
Azide	−0.08	[106]
Cytidine	−0.03	[86]
Cytosine	−0.03	[83]
Thymine	−0.02	[83]
Benzimidazole	−0.01	[107]
Carbon monoxide	−0.01	[108]
Water	−0.01	[76]
Chloride	0.00	[109]
Guanosine	0.03	[110]
Xanthosine	0.06	[83]
Thiocyanate	0.07	[76]
Hypoxanthine	0.07	[111]
Inosine	0.07	[76]
Adenosine	0.09	[86]
Pyridine	0.10	[76]
Imidazole	0.10	[76]
Benzotriazole	0.10	[107]
Adenine	0.12	[86]
Dimethylsulfide	0.12	[112]
Triphenylphosphene	0.13	[113]
Nicotinamide	0.16	[114]
Isonicotinamide	0.16	[76]
Pyrazine	0.24	[76]
Acetonitrile	0.26	[76]
Dimethylsulfoxide	0.56	[89]

understanding of the nature of the substituting ligands with respect to designing new catalytic systems to appreciate the potential range required for the particular redox reaction. An electrochemistry study of Ru(edta) complexes immobilized on the solid surface of electrodes further explores the scope of heterogenization of homogeneous catalysts[114–118] which imparts selectivity and durability to the catalytic system. Overall it appears from the results reported herein that the edta ligand can exert fine control over both the kinetics and thermodynamics of Ru(edta) mediated reactions of catalytic importance.

Table 3. Rate and activation parameters for the reduction of $[Ru^{III}(edta)(pz)]^-$ to $[Ru^{II}(edta)(pz)]^{2-}$.

R	k_r ($M^{-1}s^{-1}$)	$\Delta H^{\neq}$ (kJ mol^{-1})	$\Delta S^{\neq}$ (J mol^{-1} K^{-1})	Ref
Ascorbic acid	450	38	−122	[119]
Catechol	570			[119]
Sulfite	23	43	−73	[120]
Sulfide	50	39	−60	[121]
Cysteine	5.82	56	−44	[122]
Glutathione	3.03	55	−52	[122]

[a] at 25 °C, [b] at 30 °C

5.3 Redox Reactions of Ru(edta) Complexes

Electrochemical properties of Ru(edta) complexes discussed in the above sections clearly signify their ability to operate as potential 'molecular catalysts' for redox reactions. The $[Ru^{III}(edta)H_2O]^-$ complex reacts with the aromatic N-heterocyclic ligand, pyrazine (pz) to form the $[Ru^{III}(edta)(pz)]^-$ complex (Scheme 7). While the spectrum of $[Ru^{III}(edta)(pz)]^-$ in aqueous solution is featureless in the entire visible range,[76] its Ru(II)-analog exhibits a strong band in the visible range (λ_{max} = 462 nm, ε_{max} = 11000 M^{-1} cm^{-1}),[76] and thus offers an amenable way to monitor the electron-transfer reaction spectrophotometrically.

In this section, we discuss briefly the results of electron transfer reactions of the $[Ru^{III}(edta)(pz)]^-$ complex (pz = pyrazine) with biologically important electron donors, HR (HR = L-ascorbic acid,[119] catechol,[119] sulfite,[120] sulfide,[121] cysteine and glutathione[122]). In each case the rate of reduction of $[Ru^{III}(edta)(pz)]^-$ to $[Ru^{II}(edta)(pz)]^{2-}$ is first-order with respect to $[Ru^{III}]$. Under the specified conditions (where [R] is at least ten times in excess over $[Ru^{III}]$), values of the observed rate constant increases linearly with the increase in [R]. An outer-sphere electron transfer mechanism involving two subsequent one-electron transfer steps is proposed in Scheme 8 for the reduction of $[Ru^{III}(edta)(pz)]^-$ to $[Ru^{II}(edta)(pz)]^{2-}$ by the biologically important reducing agents, R and the corresponding rate and activation parameters are summarized in Table 3. Results and details of the earlier electron transfer studies along with the mechanistic illustrations are available in our recently published review article.[123]

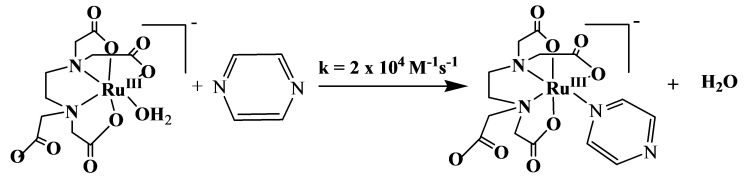

Scheme 7. Formation of $[Ru^{III}(edta)(pz)]^-$ in the reaction of $[Ru^{III}(edta)(H_2O)]^-$ with pyrazine (pz).

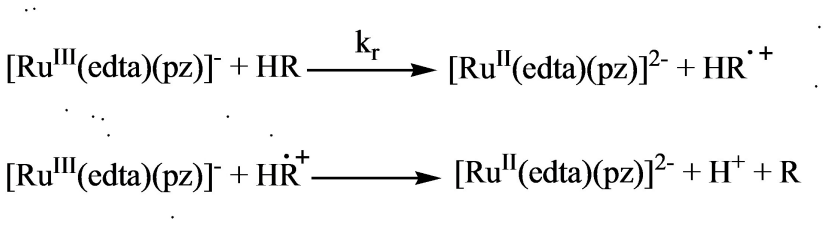

Scheme 8. Suggested mechanism for the reduction of $[Ru^{III}(edta)(pz)]^-$ by HR (HR = ascorbic acid, catechol, sulfite, sulfide, and thiols (cysteine and glutathione); R' = dehydroascorbic acid, [119] benzoquinone,[119] $S_2O_6^{2-}/HSO_4^-$, [120] S^0, [121] and CySSCy/GluSSGlu.[122]

Very recently, we have explored the ability of the $[Ru^{III}(edta)(pz)]^-$ complex in effecting redox conversion of NAD coenzymes.[124] The realization of the reversible inter-conversion between NAD^+ and NADH (Scheme 9) is a long-term challenge in biological and energy-related chemistry.

The reduction of $[Ru^{III}(edta)(pz)]^-$ by NADH was studied spectrophotometrically by monitoring the formation of red-colored $[Ru^{II}(edta)(pz)]^{2-}$ ($\lambda_{max} = 462$ nm) in aqueous solution at pH 7.0 (mes buffer).[124] However, a strict operational technique was adopted to maintain the inert atmosphere for a significantly longer period of time as the reduction of $[Ru^{III}(edta)(pz)]^-$ by NADH is slow, and the product of the reaction, $[Ru^{II}(edta)(pz)]^{2-}$ complex is extremely oxygen sensitive.[76] The reaction rate was found to be much slower ($k_r = 2.7\times10^{-2}\ M^{-1}\ s^{-1}$ at 25 °C[124]) as compared to that observed for other electron-donors (Table 3). However, the values of activation parameters ($\Delta H^{\neq} = 41\ kJ\ mol^{-1}$; $\Delta S^{\neq} = -141\ J\ mol^{-1}\ K^{-1}$) are quite comparable to the values reported for the ascorbate reduction of $[Ru^{III}(edta)(pz)]^-$ (Table 3) and consistent with the outer-sphere electron-transfer process comparable to that proposed in Scheme 5. The results of our studies elucidating the role of the $[Ru^{III}(edta)(pz)]^-$ complex in the redox conversion of NAD coenzymes via proton-coupled electron transfer reaction may shed light on designing such small molecule oxidoreductase mimics that use NAD co-enzymes for redox conversion.[125]

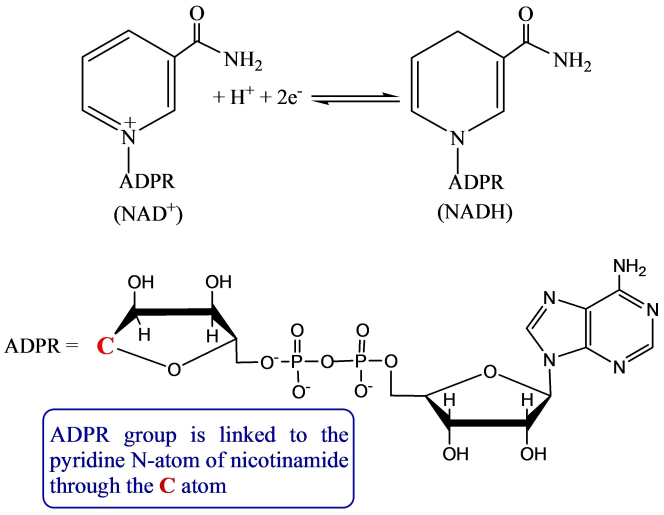

Scheme 9. Pictorial presentation of proton-coupled electron transfer reactions in redox conversion of the NAD coenzyme. Note that NAD^+ and NADH, commonly used abbreviations for the oxidized and reduced forms of the NAD coenzyme, are singly and doubly charged anions, respectively, balanced by sodium cations under physiological conditions. However, for the sake of simplicity, their formal charges are omitted in the further discussion. Reproduced from Polyhedron, 2022, 221, 115872 with permission from Elsevier.

5.4 Catalytic Significance of $Ru^{III/II}(edta)$ Complexes and Outlook

The amazing ability of $[Ru^{III}(edta)(H_2O)]^-$ towards aqua-substitution reaction, thereby enabling the activation of substrate molecules (through binding to the metal center), and the electrochemical and redox mediating properties of $[Ru(edta)L]^-$ recounted in the preceding sections are of great catalytic significance pertaining to small molecules activation in resemblance to metallo-enzymes. Our research contributions exploring the ability of the Ru(edta) complexes to mimic the activity of the oxidoreductase family of enzymes *(viz.* oxidases, peroxidases, oxygenases, and reductases) evaluating their prospect in catalytic application to chemical and electrochemical transformation of small molecules including NO generation and its utilization are systematically illustrated and reviewed recently.[77,78,126,127] Of particular importance is our very recent studies ascertaining that both the $[Ru^{II}(edta)(pz)]^{2-}$ and $[Ru^{II}(edta)(H_2O)]^{2-}$ complexes electrochemically or chemically (in the presence of electron donors) can effect oxygen reduction reaction (ORR) sequentially converting O_2 to H_2O_2 efficiently (Scheme 10).[128] Results of the above studies assume importance in the mechanistic understanding of the reduction of O_2 and H_2O_2, and thus the assessment of the prospect of such complexes in energy research.[129]

Apart from the oxygen reduction reaction,[128] the kinetic ability of $[Ru(edta)(H_2O)]^-$ towards binding bicarbonate (HCO_3^-), and nitrogen cycle intermediates, *viz.* nitrite

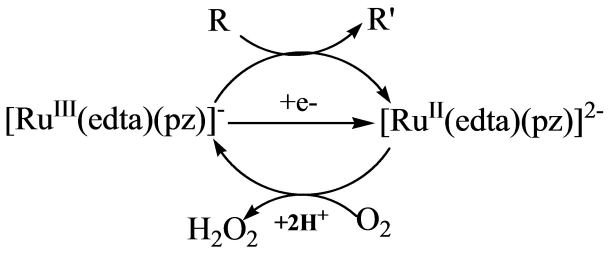

Scheme 10. Pictorial representation of $[Ru^{III}(edta)(pz)]^-$ catalyzed reduction of O_2 to H_2O_2. R = electron donating molecules; R' = oxidized product of R.

(NO_2^-), hydrazine (NH_2NH_2) and thus lowering their energy barrier for electrochemical transformation has been categorically established. Thus, there is potential for Ru(edta) complexes to act as prospective catalysts in carbon dioxide fixation,[130] and nitrogen cycle reactions.[131] It appears that the $edta^{4-}$ ligand can exert fine control over both the kinetics and thermodynamics of reactions of catalytic importance.

The results recounted in the preceding sections evidently confirm the observation that the $[Ru^{III}(edta)(H_2O)]^-$ complex due to its intrinsic lability, could easily bind to a myriad of substrates including small molecules such as H_2O_2, HCO_3^-, N-cycle intermediate molecules (via rapid substitution reactions), thus providing a lower energy pathway (rendering substantial reduction in over-potential required to initiate the electrochemical transformation of the substrate molecules directly). The wide range of metal-centered redox potentials (Table 2) may be of value in selecting the ligand of most favorable properties to design a Ru(edta)- based electron transfer catalyst for a particular redox reaction. For example $[Ru^{II}(edta)(pz)]^{2-}$ formed (via facile reduction of it Ru(III)-analog) is electrochemically competent to effect an oxygen reduction reaction.[128] It appears that the $edta^{4-}$ ligand can exert fine control over both the kinetics and thermodynamics of reactions of catalytic importance.

6. Mechanistic Information from DFT Calculations

6.1 Computer Chemistry Investigation of Ligand Exchange Reaction at Be^{2+} Complexes

Recent quantum chemistry developments allow an additional, and sometimes a different perspective on molecular chemistry topics. In combination with experimental techniques and results, they allow new and further insights so that "Computational Chemistry Investigation – The Fruitful Interplay" is a legitimate expression.[132] This connection has for many years been applied to the complex chemistry of beryllium dications. Beryllium coordination chemistry is extremely well suited for investigation by quantum chemical computations. Even if in the last 25 years some principal investigators focused on the smallest cation and various aspects of its chemistry,[133–175] the community still suffers from a complete level of understanding.

Practical research on Be^{2+} cations is a severe challenge owing to the widely known potential toxicological effects.[176–180] Computational chemistry on Be^{2+} cations benefits from the closed shell character of the beryllium dication, and that beryllium is included in most quantum chemical methods. Additional interest arises from the tetrahedral coordination of the smallest dication with a coordination number of four. A well-known coordination mode, unluckily not as thoroughly investigated as the octahedral hexa coordination metal ions with a coordination number of six. Coordination number four and solvation with standard solvent molecules allowed us to work with small Be^{2+} complexes, perfectly suited for mechanistic investigations and to be used as "guinea pigs" to explore and understand different influences on the calculated mechanism.

The first systems we investigated were water exchange at $[Be(H_2O)_4]^{2+}$, the ammonia exchange on $[Be(NH_3)_4]^{2+}$ and the hydrogen cyanide exchange on $[Be(NCH)_4]^{2+}$. Ammonia and hydrogen cyanide are of special interest, as they are so-called water-like solvents and have a long tradition in experimental chemistry.[181]

As in the case of all solvated metal ions, the reactivity of the Be^{2+} ion in solution is controlled by the lability of the coordinated solvent molecules. Already before we became interested in Be^{2+}, detailed studies on solvent-exchange reactions were performed by means of NMR techniques.[182,183] Due to the biological relevance, the most important mechanism is the exchange of coordinated water. To clarify available temperature-dependent data, Merbach *et al.*[184] applied high-pressure NMR techniques to study solvent-exchange reactions on Be^{2+}, from which activation-volume data of such processes could be obtained. The goal was to obtain a reliable mechanistic indicator that enabled an accurate description of the solvent-exchange mechanisms.[185,186] Merbach *et al.* obtained activation volumes that were interpreted as typical for a limiting associative (A) or associative-interchange (I_a) mechanism, (reported volumes of activation were found to be $[Be(H_2O)_4]^{2+}$ $-13.6\ cm^3\ mol^{-1}$) based on analogues values established by Swaddle on octahedral complexes.[187] Perhaps this linkage was not completely justified; our quantum chemical calculations appeared to challenge the linkage.

Inspired by the successful studies on solvent exchange at Li^+ with, water, ammonia, HCN, DMSO, etc.,[188–190] we focused on Be^{2+} and again the water-like solvents H_2O, NH_3 and HCN, exchanged in a similar way. In all investigations of solvent exchange studies at the Be^{2+}, center we applied the same protocol as had been used successfully on $[Li(solvent)_4]^+$. The approach was, first, the addition of an extra solvent molecule, thus indicating the calculation of the second

coordination sphere. Even if this is a highly artificial step for an ion solvation, one can learn about the system already before looking for transition states. Note, that this first step (placement of the fifth solvent molecule in the second coordination sphere) is without an implicit solvent model (e.g. CPCM or PCM in gas phase) clearly dominated by the overall charge of the complex, independently from the nature of the metal ion, more depending on the nature of the solvent molecule.

The hydrated $[Be(H_2O)_4]^{2+}$ shows tetrahedral structure with H_2O ligands in local C_{2v} symmetry indicating the domination of electrostatic ion-dipole interactions with negligible charge transfer from the O-atoms of H_2O to the dication. The effect of the two positive charges on the metal center is clearly prominent, resulting in the short Be-ligand bonds. There was no evidence of a fifth solvent molecule coordinated to the smallest cation Be^{2+}. Instead of a five-fold coordination, the second coordination sphere was preferred and possibly, hydrogen bonds were formed (see Figure 10).

The binding of the fifth water molecule in the second coordination sphere liberates 29 kcal/mol, this is exaggerated as this is in the gas phase (molten to 10% by application of the IPCM solvent model), but a clear sign of strong hydrogen bonding and leading to an activation energy of 16 kcal/mol, around 50% of the energy liberated by the addition of the fifth water molecule. Contrary to expectation if an associative (A) mechanism prevailed, no evidence was found of a five-fold coordinated Be^{2+} serving as an intermediate. In all cases, a transition state typical for an interchange (I)-type of mechanism was found.

NH_3 is a so-called water-like solvent and shows auto protolysis as does water. Therefore, ligand exchange in this solvent was investigated Again an interchange mechanism for NH_3 exchange at the $[Be(NH_3)_4]^{2+}$ center was indicated. Due to the different way of binding the fifth NH_3 molecule in the second coordination sphere by one hydrogen bond, the addition of this molecule to $[Be(NH_3)_4]^{2+}$ liberates only 21 kcal/mol, again this is molten by application of the ICPM solvent model. The activation barrier in $[Be(NH_3)_4]^{2+}$ is 18.8 kcal/mol (i.e. 3.2 kcal/mol higher than in $[Be(H_2O)_4]^{2+}$) most probably due to the more sterically demanding NH_3-ligand in comparison, and the earlier transition state compared to water exchange, visible in the more elongated distances in the cases of the entering and the leaving solvent molecules (Figure 11).

The calculations were extended to the stick-like, sterically non-demanding molecule, HCN, that is also a water-like solvent. Investigation of the HCN exchange at $[Be(NCH)_4]^{2+}$ illustrates impressively the consequence if the $[Be(NCH)_4HCN]^{2+}$ reactant state is not hydrogen bound (see in Figure 12). Immediately the energy liberated by the addition of the solvent molecule number five reduces to less than approximately 50% of the values found in the corresponding cases of water and ammonia, and the activation energies are only around 30% of those for NH_3 and H_2O. The difference between the H-bonded and the ligand exchange process of those starting structure at $[Be(NCH)_4]^{2+}$, is 7.4 kcal/mol (see Table 4).

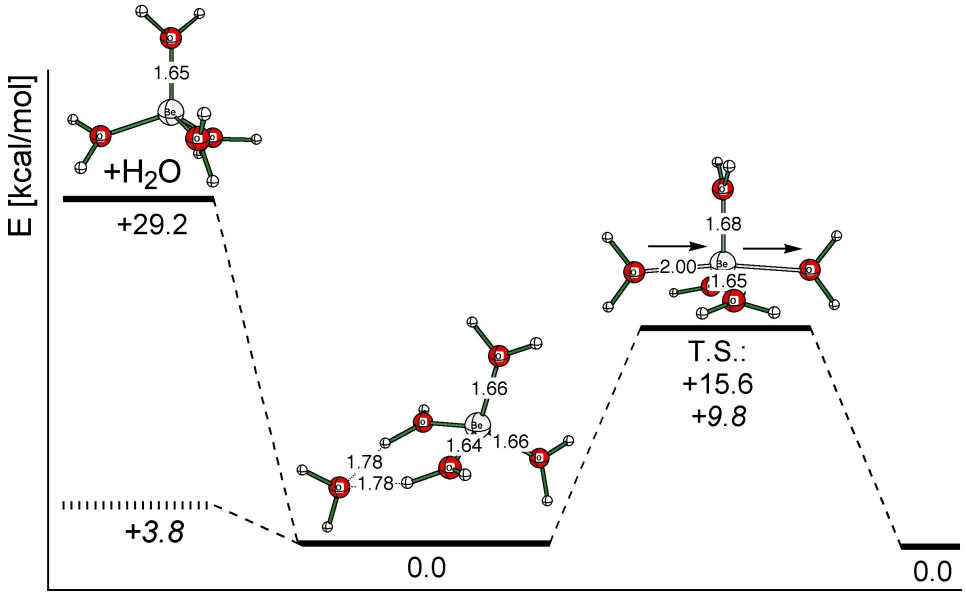

Figure 10. Calculated water exchange at $[Be(H_2O)_4]^{2+}$ (values; B3LYP/6-311+G**+ ZPE(B3LYP/6-311+G**), italic: *B3LYP/6-311+G**(IPCM)// B3LYP/6-311+G**+ ZPE(B3LYP/6-311+G**)*.

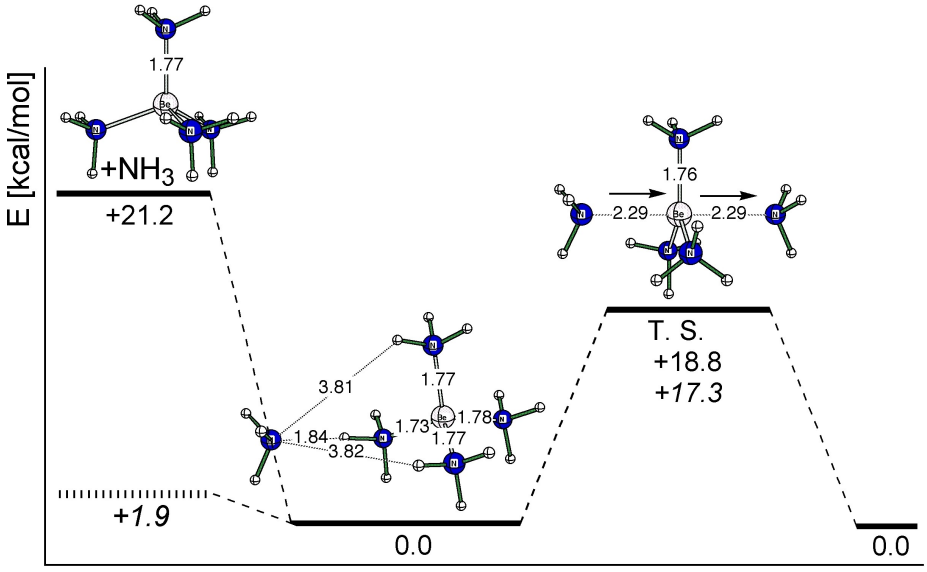

Figure 11. Calculated ammonia exchange at $[Be(NH_3)_4]^{2+}$ (values; B3LYP/6-311+G**+ ZPE(B3LYP/6-311+G**), italic: *B3LYP/6-311+G**(IPCM)//B3LYP/6-311+G**+ZPE(B3LYP/6-311+G**)*.

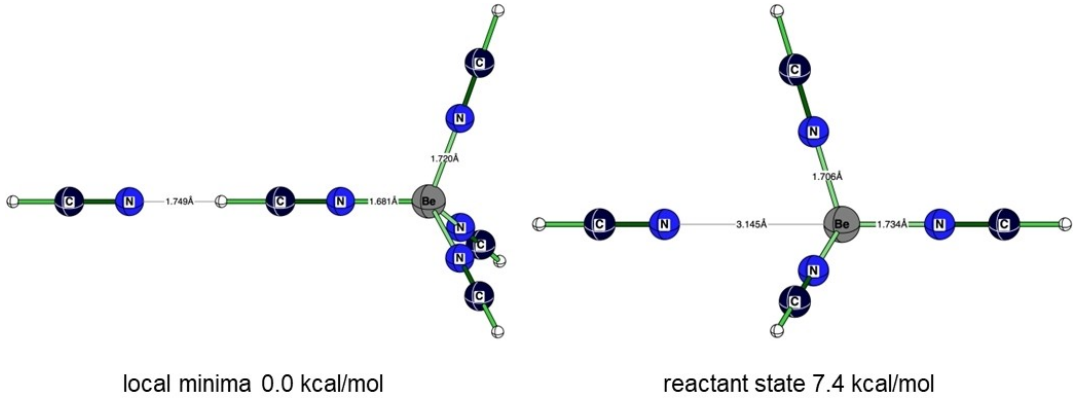

Figure 12. Energetic comparison (B3LYP/6-311+G**) of the hydrogen bound HCN and the starting structure for the ligand exchange at $[Be(NCH)_4]^{2+}$.

In recent years new quantum chemical methods appeared and were applied, but with these three elementary reactions a stock of reliable reference data has been accumulated, that could be applied for further calculations, such as challenging methods or step by step modification in a controlled manner for the systems of interest.

A central problem in calculating solvent exchange reactions is of course the treatment of the bulk solvents. The goal was and still is to investigate these types of reactions in a simple, clear, and well-arranged way, so non-dynamic protocols and techniques were continued. The simplest way to include the influence of solvent effects in quantum chemical calculations is the use of implicit solvent models. While energy calculations on the exact characterized gas-phase structures work well, (*I*) efforts failed to obtain local minima for the reactant state while optimizing them. This is not a very convenient situation. An alternative approach would be to concentrate on the entering and the leaving water molecules in $[Be(H_2O)_4]^{2+}$ by a fifth water molecule.[195] Independently, if simple gas phase calculations were applied with 4+1 water molecules (see Figure 13), if DFT or Post-HF-techniques were applied, including different sorts of implicit solvent models or added another 5 water molecules to concatenate the entering and the leaving water ligand, an I_a mechanism was always obtained; of course, the activation energy varied as expected. As the interest is in understanding mechanistic pathways and influences on the mechanism this consistent reproduction of the *I*-mechanism as

Table 4. Overview of a Be^{2+} ligand exchange reactions at different theory levels, in kcal/mol.

Solvent: H_2O	Ref.	$[BeSol_4]^{2+}$ + Sol	$[Be(Sol)_4Sol]^{2+}$	TS
B3LYP/6-311 + G**	[191]	+29.2	0.0	+15.6
MP2(full)/6-311 + G**//B3LYP/6-311 + G**	[191]	+29.3	0.0	+12.6
B3LYP(IPCM)/6-311 + G**//B3LYP/6-311 + G**	[191]	+3.8	0.0	+9.8
B3LYP(CPCM)/6-311 + G**//B3LYP/6-311 + G**	[192]	−2.5	0.0	+10.3
ωB97XD/6-311 + G**	[193]	+30.2	0.0	+13,0
G3		+30.2	0.0	+13.3
Solvent: NH_3				
B3LYP/6-311 + G**	[191]	+21.2	0.0	+18.8
MP2(full)/6-311 + G**//B3LYP/6-311 + G**	[191]	+21.8	0.0	+15.8
B3LYP(IPCM)/6-311 + G**//B3LYP/6-311 + G**	[191]	+1.9	0.0	+17.3
ωB97XD/6-311 + G**	[191]	+22.8	0.0	+15.4
Solvent: HCN				
B3LYP/6-311 + G**	[191]	+12.7	0.0	+4.3
MP2(full)/6-311 + G**//B3LYP/6-311 + G**	[191]	+16.3	0.0	+1.5
B3LYP(IPCM)/6-311 + G**//B3LYP/6-311 + G**	[191]	−4.1	0.0	+3.9
ωB97XD/6-311 + G**	[194]	+15.2	0.0	+2.5
G3		+15.6	0.0	+5.8
Solvent: Pyridine				
ωB97XD/6-311 + G**	[191]	+18.3	0.0	+11.8
Solvent: H_2S				
ωB97XD/6-311 + G**	[194]	+14.5	0.0	+12.0
Solvent: H_2Se				
ωB97XD/6-311 + G**	[191]	+13.3	0.0	+12.0

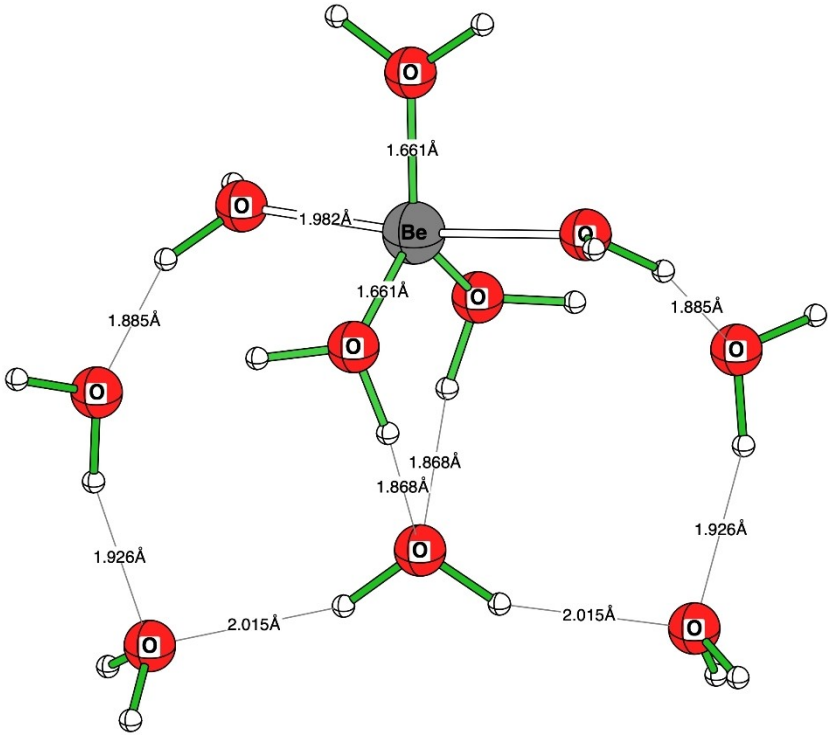

Figure 13. Calculated transition state (B3LYP/6-311 + G**) for the water exchange at $[Be(H_2O)_4]^{2+}$ with concatenated entering and leaving water ligands.

described, led to the conviction that the simple and small model applied is suitable for our purpose.

The next step was to investigate the influence on solvent exchange of spectator ligands. Three sorts of monodentate ligands neutral,[194] anionic[192], and cationic,[196] that serve as spectator ligands coordinated to the beryllium dication were investigated, these do not participate in the ligand exchange process themselves.

To learn about the influence of neutral ligands, the water exchange rate for $[BeL(H_2O)_3]^{2+}$ was calculated. As ligands, L around 35 neutral molecules with donor atoms from main groups V and VI, and different hybridization, were selected. In all cases, similar data were obtained. The addition within the calculation of the fourth water molecule liberated yielded on average −27 kcal/mol (B3LYP/6-311 + G**), while the activation energy was averaged at 17 kcal/mol (B3LYP/6-311 + G**). The large difference due to the trans-influence and trans-effect observed in square-planar complexes, in comparison to tetrahedrally coordinated cases, is understandable since there are no joined orbitals that are affected by the spectator ligand and so this is only an aspect for systems with d-orbitals involved in bonding.[194]

In the next step, neutral ligands were substituted by mono anionic ligands to test the influence of a negative charge on the water exchange mechanism, reducing the overall charge from 2+ to 1+. Therefore, L: H^-, F^-, Cl^-, Br^-, OH^- were introduced, and as a result of developing interest in ionic liquids the effect of NC-N^--CN on water exchange at $[BeL(H_2O)_3]^+$ was tested. As expected, the energy set free by binding an additional water molecule to $[BeL(H_2O)_3]^+$ to obtain $[BeL(H_2O)_3H_2O]^+$ to 60% (17 kcal/mol (B3LYP/6-311 + G**)) of the value of the dicationic species. A value was still 5 kcal/mol higher as in the case of $[Li(H_2O)_4]^+$.[197] The averaged transition state passed during the water exchange at $[BeL(H_2O)_3]^+$ is, with 12 kcal/mol (B3LYP/6-311 + G**) also reduced (20%) from the value for $[Be(H_2O)_4]^{2+}$. This effect can be attributed to the higher electron density at the beryllium cation due to the anionic ligand L.[192]

If anionic ligands L decrease the accretion energy of the extra water molecule and to a smaller degree the activation energy, then cationic ligands should increase the energetic values. An outstanding group of ligands was designed, inspired by the SASAPHOS protocol[198] of Robert Weiss and team; starting from simple deprotonated para-hydroxopyridine and pyridine, up to three pyridinium moieties were added to pyridine. In this way we were able to cover a series of ligands L from mono-anionic to tricationic systems allowing the range from $[BeL(H_2O)_3]^+$ to $[BeL(H_2O)_3]^{5+}$. As anticipated, a linear correlation between the charge of the complex and the accretion energy of the extra water molecule (binding energy) was obtained: furthermore, the activation energy ($[BeL(H_2O)_3]^+$: −18.0 kcal/mol/ + 11.2 kcal/mol $[BeL(H_2O)_3]^{5+}$: −39.0 kcal/mol/ + 23.6 kcal/mol (B3LYP/6-311 + G**)) increased linearly.[196]

Besides challenging modifications of the coordination sphere within the solvent complexes, they can be used to challenge quantum chemical methods including their applicability and predictive power. While theoretical chemistry can often reach different conclusions in similar goals as experimental chemistry, the discrimination between I_a, I, and I_d mechanisms often remains a problem. As test cases, we calculated the solvent exchange at $[Be(Sol)_4]^{2+}$ (Sol: H_2O, H_2S. H_2Se, HCN, pyridine, and NH_3) to have different hybridized N-atoms and coordinating lone pairs of different quantum numbers. An expectation from orientating calculations is that these factors can shift an I-mechanism for I_a to I_d.

While experimentalists can differentiate between I_a and I_d by the experimental activation volume, quantum chemical studies traditionally utilize differences in bond length as descriptors.[199,200] Analysing the electron density (ρ) between the beryllium dication and the donor atom of the entering or leaving ligand offers a quantum chemical bond approach in relation to discrimination between I_a and I_d mechanism. Analogous to the increasing bond length the electron density (ρ) decreases, a clear sign of a more dissociative character (Figure 14).

A central question in every reaction is, when does bond formation start? An interesting method for atoms within molecules (AIM) is to perform an analysis. Here we used the HCN exchange on $[Be(NCH)_4]^{2+}$ utilizing a small molecular system to investigate the known reaction mechanism. After optimization at 0.05 Å steps along the reaction coordinate, topological analysis using QTAIM demonstrates the change in electron density ρ at the transition from a coordinating interaction (presence of bond critical points BCP) to a non-coordinative interaction (presence of cage critical points CCP to equatorial HCN molecules). At approximately 2.3 Å an interaction between Be^{2+} and the incoming/leaving NCH ligand is observed. At this distance, the CCPs between Be^{2+} and NCH molecules change into BCPs. Therefore, this distance could be best addressed as the first contact point (FCP) of this reaction (see Figure 15).[193]

6.2 Computer Chemistry Investigation of Ligand Exchange Reaction at Ru(II) Complexes

Understanding the reactivity of Ru(II) polypyridyl complexes is important in terms of their potential biological applications in particular, anti-tumor activity[201–207] and their role in the redox biology of cells.[208–211] Such Ru(II) complexes are prodrugs that are activated via the aquation of the chloride ligand. More recent studies have focused on their aqueous chemistry, substitution behavior, possible role as anti-tumor reagents,[202,212] and catalytic role in water oxidation

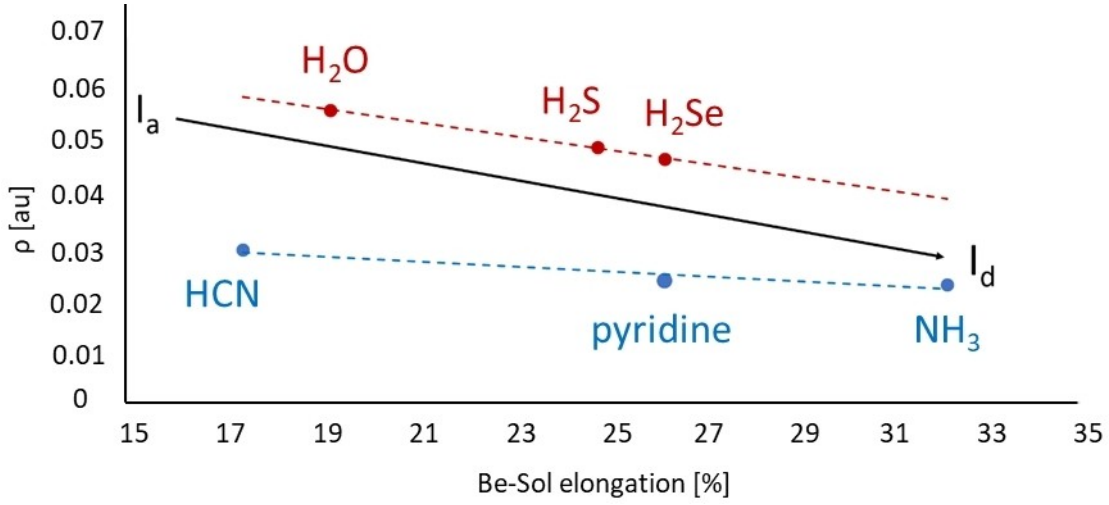

Figure 14. AIM based analysis of the electron density ρ for solvent exchange reactions at $[Be(Sol)_4]^{2+}$ (Sol: H_2O, H_2S, H_2Se, HCN, pyridine, NH_3) (ωB97XD/6-311+G**) AIMAll V17.[193]

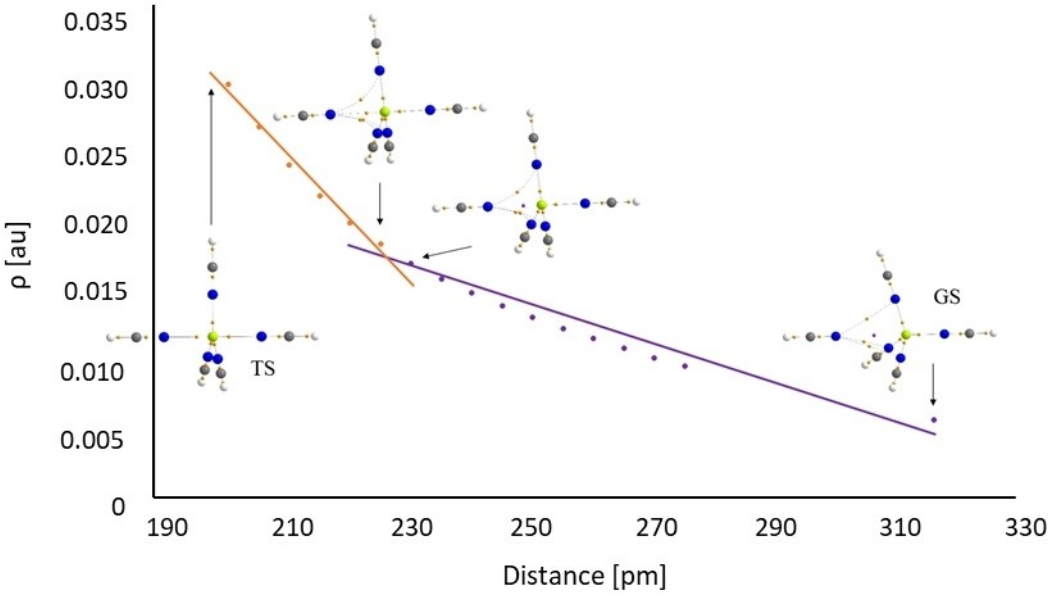

Figure 15. AIM analysis of the HCN exchange at $[Be(NCH)_4]^{2+}$ (BCP: orange dots, CCP: violet dots) (ωB97XD/6-311+G**) AIMAll V17.[193]

reactions.[213–218] It was observed that chelates affect the lability of the complexes through the σ donor and π back-bonding effects which significantly affect the electrophilicity of the metal center and in turn the substitution behavior of such complexes.[219–222] Consequently it is found that Ru(II) complexes containing an aliphatic amino ligand near the metal reaction center react much faster in all the aquation and substitution reactions studied than when the Ru(II) complexes contain an aromatic amino ligand.[223,224] This has consequences for the eventual biological application of these complexes. Therefore, since the nature of the spectator chelate has a pronounced effect on the stability and in general on the aqueous behavior of such complexes comparing the mechanistic insight obtained from classical kinetic studies with that obtained from DFT calculations can provide further insight into their reaction kinetics.

The importance of the labile ligands in fine-tuning the reactivity of the polypyridyl Ru(II) complexes has been best demonstrated in work by Charzanowska *et al.*[224] on two aqua complexes $[Ru^{II}(terpy)(bipy)H_2O]^{2+}$ and $[Ru^{II}$-

$(terpy)(en)H_2O]^{2+}$ (where terpy = 2,2':6',2''-terpyridine, bipy = 2,2'-bipyridine and en = ethylenediamine) where selected ligand chelates can affect the lability of metal centers through different σ donor and π back-bonding effects. The data they gathered indicate very similar rate and activation parameters for the reactions of those aqua complexes with chloride, thiourea, and cyanide as entering ligands, demonstrating that these complexes show a low nucleophilic discrimination ability. With respect to their lability, the $[Ru^{II}(terpy)(en)H_2O]^{2+}$ complex is *ca.* 30–60 times more labile than the $[Ru^{II}(terpy)(bipy)H_2O]^{2+}$ complex in a process of a previous aquation of a chloride complex and further anation reactions with chloride, thiourea or cyanide. The reactivity ratio of the $[Ru^{II}(terpy)(en)H_2O]^{2+}$ to the $[Ru^{II}(terpy)(bipy)H_2O]^{2+}$ complex of 1 : 64 for the aquation reaction, 1 : 30 for anation by chloride and 1 : 64 for anation by thiourea. This occurrence can be accounted for in terms of π back-bonding effects of the bipy chelate as compared to the en ligand that will increase the electrophilicity of the Ru(II) complex and change its electronic nature more in the direction of the less labile Ru(III) complex. For comparison, water exchange on the studied $[Ru^{II}(terpy)(en)H_2O]^{2+}$ and $[Ru^{II}(terpy)(bipy)H_2O]^{2+}$ complexes, showed that the observed rate constants are, within experimental error, approximately 50 times faster than that reported for $[Ru(H_2O)_6]^{2+}$.[225] This clearly showed the donor chelate effect of the polypyridyl ligands in the labialization of the coordinated water molecule. The activation parameters for the $[Ru^{II}(terpy)(en)H_2O]^{2+}$ and $[Ru^{II}(terpy)(bipy)H_2O]^{2+}$ complexes anation reactions, especially the activation entropy and activation volume data, clearly support an associative interchange (I_a) mechanism. Furthermore, in the case of the substitution of coordinated water by thiourea the observed activation volume is more negative, i. e. more associative in the case of the $[Ru^{II}(terpy)(bipy)H_2O]^{2+}$ complex, which can be due to the higher electrophilicity expected for the Ru(II) center. Quantum chemical calculations can aid in obtaining more detailed insight into the water exchange mechanism of these complexes at the molecular level. For the water exchange reaction (at B3LYP/def2svp theory level) for the $[Ru^{II}(terpy)(bipy)H_2O]^{2+}$ complex, the entering water molecule in the ground state is in the second coordination sphere and moves significantly closer to the metal center at a distance of 3.13 Å, which is approximately halfway to the metal center for a bonding distance of 2.18 Å. At the same time the coordinated water molecule in the ground state moves away from the metal center to a distance of 3.26 Å, such that the transition state is almost symmetrical, typical for a pure interchange (I) water exchange mechanism. In the case of the water exchange reaction on the $[Ru^{II}(terpy)(en)H_2O]^{2+}$ complex, the entering water molecule in the ground state can either attach close to the leaving water molecule at a distance of 4.18 Å (d(Ru–OH_2···OH_2) 1.64 Å), similar to that found for the $[Ru^{II}(terpy)(bipy)H_2O]^{2+}$ complex, or bind via a hydrogen bond to the N–H group of the $[Ru^{II}(terpy)(en)H_2O]^{2+}$ complex at a distance of 1.93 Å (d(Ru···OH_2) 4.46 Å). The structure where the hydrogen bond between the N–H group and the entering water molecule is around 3 kcal mol^{-1} are more stable than the structure where the entering water is bound to the leaving moiety (the energy values are related to B3LYP(CPCM)/def2tzvp and ωB97XD(CPCM)/def2tzvp energy calculations on the B3LYP/def2svp structures). It appears that in the case of the $[Ru^{II}(terpy)(en)H_2O]^{2+}$ complex, the presence of the amine group seems to assist the water exchange mechanism by lowering the activation energy barrier. Therefore, besides the electronic effect (σ donor and π back-bonding) and not neglecting the omnipresent steric hindrance of the spectator chelate ligand that could also contribute to the reactivity trend, the influence of the possible hydrogen bond formation between the spectator and the entering ligand could also contribute to the fine-tuning of the Ru(II) complexes reactivity. This effect can be best demonstrated in the case of $[Ru^{II}(terpy)(ampy)H_2O]^{2+}$ complex (terpy = 2,2':6',2''-terpyridine and ampy = 2-(aminomethyl)pyridine) where the ampy ligand has a possibility to occupy two different positions in the complex, denying (Figure 16a) or allowing (Figure 16b) the possibility of a hydrogen bond formation with the entering ligand near the reaction center.

Crystallographic X-ray analysis has identified the formation of a $[Ru^{II}(terpy)(ampy)H_2O]^{2+}$ complex with the positioning of the ampy ligand preventing the formation of the hydrogen bond to the entering ligand (Figure 16a).[226] Nevertheless, quantum chemical calculations have shown that the energy barrier of the water exchange reaction is 2.67 kcal/mol lower when a hydrogen bond is participating in the reaction process (the energy values are related to ωB97XD/def2tzvp energy calculations on the B3LYP/def2svp structures). This lowering of the energy barrier regarding the orientation of the ampy ligand is also observed in the water substitution by thiourea, where substituting water with thiourea is by 2 kcal/mol more kinetically favorable in the case of $[Ru^{II}(terpy)(ampy)H_2O]^{2+}$ (*a*) than in the case of a (*b*) complex (Figure 16).[223] For a much wider series of Ru(II) complexes (Figure 17), Ćoćić *et al.*[223] compared the mechanistic behavior obtained from classical kinetic studies with the DFT calculations in order to gain insight into the underlying reaction mechanisms on the water exchange reactions.

The positions of the leaving and the entering water molecules in the transition state for a series of complexes, presented in Figure 17, were all within the range expected for a single transition state within the concept of an associative interchange (I_a) mechanism, therefore supporting the experimental finding of a reaction mechanism. The arrangement of the entering water molecule in a water exchange reaction for

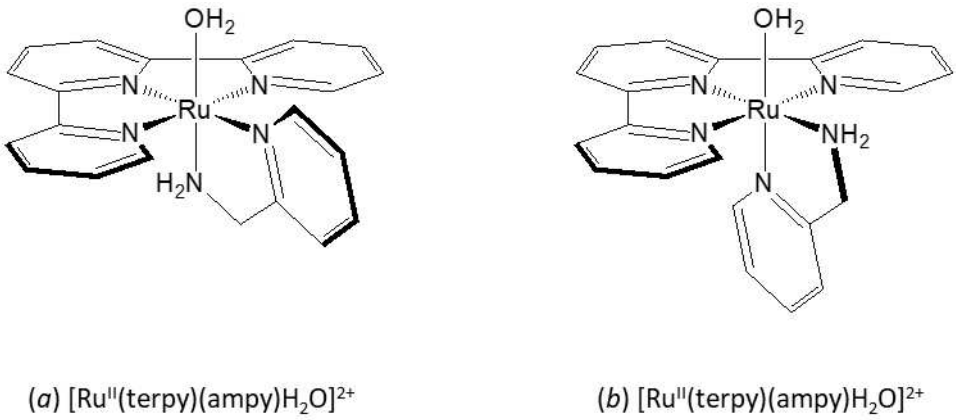

Figure 16. Schematic structures $[Ru^{II}(terpy)(ampy)H_2O]^{2+}$ complexes.

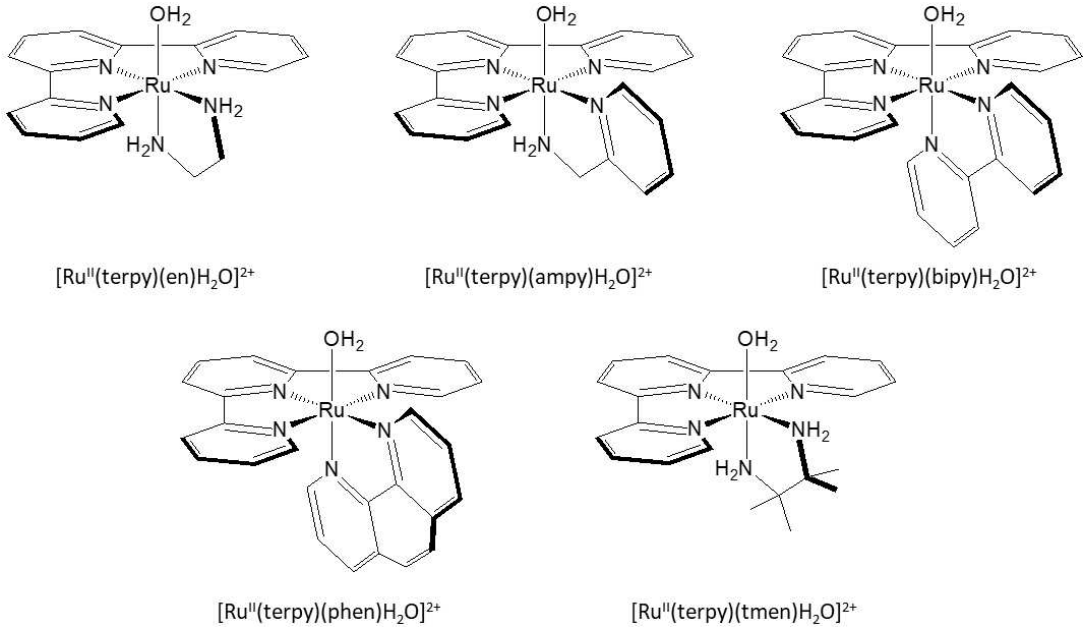

Figure 17. Schematic structures of the $[Ru^{II}(terpy)(NN)H_2O]^{2+}$ complexes (terpy = 2,2':6',2''-terpyridine, en = ethylenediamine, ampy = 2-(aminomethyl)pyridine, bipy = 2,2'-bipyridine, phen = 1,10-phenanthroline, tmen = N,N,N',N'-tetramethylethylenediamine).

complexes in Figure 11 results in formation of the relatively symmetrical transition states, which are typical for an interchange (*I*) water exchange mechanism. However, this arrangement changes in the case of the $[Ru^{II}(terpy)(en)H_2O]^{2+}$ complex in which the entering water molecule is located between the ethylenediamine ligand and the coordinated water molecule, forming an additional hydrogen bond with the N–H group. The distance of the entering water molecule to the Ru^{II} center (3.04 Å) is shorter than the distance of the leaving water molecule (3.31 Å), which is reflected in the transition state energy Table 5.

A comparison of the energy of the transition states displayed, in Table 2, of complexes presented in Figure 17, where complex $[Ru^{II}(terpy)(tmen)H_2O]^{2+}$ has no ability to form a similar type of additional hydrogen bond, the TS energy of $[Ru^{II}(terpy)(en)H_2O]^{2+}$ is 4.42 kcal/mol lower. Thus, the ability to form an additional hydrogen bond with the inert spectator ligand of a complex close to the reaction center has a "slingshot" effect on the overall water exchange reaction. In a report of Ćoćić *et al*[227] these "slingshot" effects were studied in detail by applying conceptual density functional theory,[228] and the concept of this reaction mechanism was put on a quantitative basis. The results enable the

Table 5. Calculated energies (ωB97XD/def2tzvp//B3LYP/def2svp + ZPE(B3LYP/def2svp)) for the water exchange reactions of the aqua complexes presented in Figure 17.

Complex	TS/E(kcal/mol)	d_e[a)] [Å]	d_l[b)] [Å]
[en-H_2O]	19.34	3.04	3.31
[ampy-H_2O]	21.06	3.23	3.16
[bipy-H_2O]	20.40	3.27	3.13
[phen-H_2O]	20.37	3.11	3.24
[tmen-H_2O]	23.76	3.30	3.28

[a)] Distance between Ru^{II}-center and the oxygen of the entering water in the transition state
[b)] Distance between the Ru^{II}-center and the oxygen of the leaving water in the transition state

characterization of the significant influence of an intermolecular hydrogen bond formed between the entering and the spectator ligand where the overall reaction energy barrier can be lowered by 5~10 kcal/mol, details that should be taken into account in designing suitable complexes for desirable reaction behavior as in catalytic processes and biomedical application.

7. Summary

In this review, we have summarized the main mechanistic conclusions dealing with inorganic reaction mechanisms. Colin Hubbard wrote the Introduction. The first theme was centered on nitrosylcobalamin and its reactions, and was written by Justyna Polaczek. The next theme covered various aspects of microperoxidase-11 and its chemistry, and was written by Konrad Kieca, Maria Oszajca and Grażyna Stochel. Subsequently, Olga Impert and Anna Katafias presented a detailed report on mixed-valence Ru(II)/Ru(III) ion-pair complexes and their chemistry coupled to solid state structures. The next section dealt with the reactivity of Ru(III/II)(edta) complexes: kinetic lability and redox ability, and was written by Debabrata Chatterjee. Dušan Ćoćić and Ralph Puchta presented a DFT account on computer chemistry investigation of ligand exchange reactions at Be^{2+} complexes. Subsequently, the same authors presented an account of computer chemistry investigation of ligand exchange reaction at Ru^{2+} complexes.

The corresponding author sincerely appreciates the help of Konrad, Marysia, and Justyna for tackling the revision of the manuscript and putting it into an acceptable format! All other authors are thanked for their sincere collaboration to put this review together! I really appreciate all your efforts and can only say 'Thank you very much for this Team work'!

On a final note, we would like to congratulate Toni Neubrandt, Achim Zahl, Carlos Dücker-Benfer, Ursula Palmer, and Susanne Hoffmann on the occasion of their 60th birthdays.

Acknowledgements

KK, GS, MO, JP and RvE acknowledge financial support from the National Science Centre in Poland, Grant No. 2019/35/B/ST4/04266 and Grant No. 2016/23/D/ST4/00303, respectively. D.Ć. thanks the Ministry of Education, Science and Technological Development of the Republic of Serbia (Agreement No. 451-03-47/2023-01/200122). We thank Johannes Endres, TH Nuremberg for technical support, Prof. Tim Clark and Prof. Petra Imhof for hosting this work at the CCC and the Regionales Rechenzentrum Erlangen (RRZE) for a generous allotment of computer time. All of the authors thank their co-workers and collaborators who have contributed to this study. Open Access funding enabled and organized by Projekt DEAL.

Conflict of Interest

The authors declare no conflict of interest.

Data Availability Statement

The data that support the findings of this study are available on request from the corresponding author. The data are not publicly available due to privacy or ethical restrictions.

References

[1] R. van Eldik, "List of Papers" can be found under https://www.chem.umk.pl/panel/wp-content/uploads/Papers-Rudi-van-Eldik.pdf, 2023.
[2] M. Wolak, A. Zahl, T. Schneppensieper, G. Stochel, R. van Eldik, *J. Am. Chem. Soc.* **2001**, *123*, 9780–9791.
[3] H. Subedi, H. A. Hassanin, N. E. Brasch, *Inorg. Chem.* **2014**, *53*, 1570–1577.
[4] H. A. Hassanin, L. Hannibal, D. W. Jacobsen, M. F. El-Shahat, M. S. A. Hamza, N. E. Brasch, *Angew. Chem. Int. Ed.* **2009**, *48*, 8909–8913.
[5] J. Polaczek, L. Orzel, G. Stochel, R. van Eldik, *J. Biol. Inorg. Chem.* **2015**, *20*, 1069–1078.
[6] J. Polaczek, Ł. Orzeł, G. Stochel, R. van Eldik, *J. Biol. Inorg. Chem.* **2018**, *23*, 377–383.
[7] J. Polaczek, H. Subedi, Ł. Orzeł, L. Lisboa, R. B. Cink, G. Stochel, N. E. Brasch, R. van Eldik, *Inorg. Chem.* **2021**, *60*, 2964–2975.
[8] O. Piloty, *Ber. Dtsch. Chem. Ges.* **1896**, *29*, 1559–1567.
[9] K. M. Miranda, *Coord. Chem. Rev.* **2005**, *249*, 433–455.
[10] C. D. Hubbard, D. Chatterjee, M. Oszajca, J. Polaczek, O. Impert, M. Chrzanowska, A. Katafias, R. Puchta, R. van Eldik, *Dalton Trans.* **2020**, *49*, 4599–4659.
[11] J. Polaczek, G. Stochel, R. van Eldik, *Eur. J. Inorg. Chem.* **2021**, *2021*, 2325–2333.

[12] J. Polaczek, A. Jodłowska, G. Stochel, R. van Eldik, *Atmosphere* **2021**, *12*, 1050.
[13] J. Polaczek, G. Stochel, D. Ruiz Molina, F. Novio Vázquez, R. van Eldik, *Polyhedron* **2022**, *223*, 115942.
[14] S. A. Suárez, M. A. Martí, P. M. De Biase, D. A. Estrin, S. E. Bari, F. Doctorovich, *Polyhedron* **2007**, *26*, 4673–4679.
[15] N. Lehnert, E. Kim, H. T. Dong, J. B. Harland, A. P. Hunt, E. C. Manickas, K. M. Oakley, J. Pham, G. C. Reed, V. S. Alfaro, *Chem. Rev.* **2021**, *121*, 14682–14905.
[16] P. C. Ford, *Inorg. Chem.* **2010**, *49*, 6226–6239.
[17] Ł. Orzeł, M. Oszajca, J. Polaczek, D. Porębska, R. van Eldik, G. Stochel, *Molecules* **2021**, *26*.
[18] A. Franke, M. Oszajca, M. Brindell, G. Stochel, R. van Eldik, *Adv. Inorg. Chem.* **2015**, *67*, 171–241.
[19] A. D. Carraway, R. S. Burkhalter, R. Timkovich, J. Peterson, *J. Inorg. Biochem.* **1933**, *52*, 201–207.
[20] C. Veeger, *J. Inorg. Biochem.* **2002**, *91*, 35–45.
[21] H. M. Marques, *Dalton Trans.* **2007**, 4371–4385.
[22] E. Gkaniatsou, C. Serre, J. P. Mahy, N. Steunou, R. Ricoux, C. Sicard, *J. Porphyrins Phthalocyanines* **2019**, *23*, 1–11.
[23] A. Riposati, T. Prieto, C. S. Shida, I. L. Nantes, O. R. Nascimento, *J. Inorg. Biochem.* **2006**, *100*, 226–238.
[24] P. Ascenzi, D. Sbardella, R. Santucci, M. Coletta, *J. Biol. Inorg. Chem.* **2016**, *21*, 511–522.
[25] V. S. Sharma, R. A. Isaacson, M. E. John, M. R. Waterman, M. Chevion, *Biochemistry* **1983**, *22*, 3897–3902.
[26] V. S. Sharma, H. M. Ranney, J. F. Geibel, T. G. Traylor, *Biochem. Biophys. Res. Commun.* **1975**, *66*.
[27] M. Oszajca, G. Drabik, M. Radoń, A. Franke, R. van Eldik, G. Stochel, *Inorg. Chem.* **2021**, *60*, 15948–15967.
[28] A. D. Carraway, M. G. Mccollum, J. Peterson, *Inorg. Chem.* **1996**, *35*, 6855–6891.
[29] D. Verbaro, A. Hagarman, A. Kohli, R. Schweitzer-Stenner, *J. Biol. Inorg. Chem.* **2009**, *14*, 1289–1300.
[30] H. M. Marques, C. B. Perry, *J. Inorg. Biochem.* **1999**, *75*, 28–29.
[31] T. Mashino, S. Nakamura, M. Hirobe, *Tetrahedron Lett.* **1990**, *31*, 3163–3166.
[32] M. T. Wilson, R. J. Ranson, P. Masiakowski, E. Czarnecka, M. Brunori, *Eur. J. Biochem.* **1977**, *77*, 193–199.
[33] E. Katz, R. Baron, I. Willner, *J. Am. Chem. Soc.* **2005**, *127*, 4060–4070.
[34] X. Zhu, I. Yuri, X. Gan, I. Suzuki, G. Li, *Biosens. Bioelectron.* **2007**, *22*, 1600–1604.
[35] P. Ascenzi, D. Sbardella, M. Fiocchetti, R. Santucci, M. Coletta, *J. Inorg. Biochem.* **2015**, *153*, 121–127.
[36] P. Ascenzi, G. De Simone, D. Sbardella, M. Coletta, *J. Biol. Inorg. Chem.* **2019**, *24*, 21–29.
[37] M. Oszajca, A. Jodłowska, D. Rutkowska-Żbik, K. Kieca, G. Stochel, *Inorg. Chem.* **2023**, *62*, 5630–5643.
[38] V. Fernando, X. Zheng, Y. Walia, V. Sharma, J. Letson, S. Furuta, *Antioxidants* **2019**, *8*, 404.
[39] J. S. Stamler, S. Lamas, F. C. Fang, *Cell* **2001**, *106*, 675–683.
[40] J. Sun, C. Steenbergen, E. Murphy, *Antioxid. Redox Signaling* **2006**, *8*, 1693–1705.
[41] E. Nagababu, *Free Radical Biol. Med.* **2016**, *101*, 296–304.
[42] G. Reichenbach, S. Sabatini, R. Palombari, C. A. Palmerini, *Nitric Oxide* **2001**, *5*, 395–401.
[43] S. Basu, A. Keszler, N. A. Azarova, N. Nwanze, A. Perlegas, S. Shiva, K. A. Broniowska, N. Hogg, D. B. Kim-Shapiro, *Free Radical Biol. Med.* **2010**, *48*, 255–263.
[44] A. Weichsel, E. M. Maes, J. F. Andersen, J. G. Valenzuela, T. K. Shokhireva, F. A. Walker, W. R. Montfort, *Proc. Natl. Acad. Sci. USA* **2005**, *102*, 594–599.
[45] W. H. Koppenol, *Inorg. Chem.* **2012**, *51*, 5637–5641.
[46] M. Đurović, M. Oszajca, G. Stochel, R. van Eldik, *Eur. J. Inorg. Chem.* **2018**, 1229–1235.
[47] W. Kaim, B. Sarkar, *Coord. Chem. Rev.* **2007**, *251*, 584–594.
[48] A. S. Hazari, A. Indra, G. K. Lahiri, *RSC Adv.* **2018**, *8*, 28895–28908.
[49] P. J. Low, *Angew. Chem. Int. Ed.* **2023**, *62*, e202217082.
[50] C. Creutz, H. Taube, *J. Am. Chem. Soc.* **1973**, 1086–1094.
[51] C. P. Raptopoulou, V. Psycharis, *Inorg. Chem. Commun.* **2008**, *11*, 1194–1197.
[52] S. Manna, A. Bhunia, S. Mistri, J. Vallejo, E. Zangrando, H. Puschmann, J. Cano, S. C. Manna, *Eur. J. Inorg. Chem.* **2017**, *2017*, 2585–2594.
[53] X. M. Chen, H. A. Chen, B. M. Wu, T. C. W. Mak, *Acta Crystallogr. Sect. C* **1996**, *52*, 2693–2695.
[54] G. O. Egharevba, M. Mégnamisi-Bélombé, H. Endres, E. Rossato, *Acta Crystallogr. Sect. B* **1982**, *38*, 2901–2903.
[55] L. R. Nassimbeni, G. C. Percy, A. L. Rodgers, *Acta Crystallogr. Sect. B* **1976**, *32*, 1252–1256.
[56] B. Das, J. B. Baruah, *Inorg. Chem. Commun.* **2010**, *13*, 350–352.
[57] R. Hämäläinen, U. Turpeinen, *Acta Chem. Scand.* **1989**, *13*, 15–18.
[58] Brown D. B., Wrobleski J. T., in *Mixed-Valence Compounds*, **1980**, p. 49.
[59] A. Panja, N. C. Jana, S. Adak, K. Pramanik, *Inorg. Chim. Acta* **2017**, *459*, 113–123.
[60] F. L. Yin, R. Xie, J. Hao, Y. F. Wang, J. J. Yang, *Inorg. Chem. Commun.* **2013**, *30*, 97–104.
[61] Z.-J. Ouyang, X.-Y. Mo, J.-Q. Ye, X.-X. Yu, S.-Y. Huang, X.-L. Liu, W.-B. Chen, S. Gao, W. Dong, *Dalton Trans.* **2021**, *50*, 5960–5967.
[62] O. Impert, A. Kozakiewicz, G. Wrzeszcz, A. Katafias, A. Bieńko, R. van Eldik, A. Ozarowski, *Inorg. Chem.* **2020**, *59*, 8609–8619.
[63] G. M. Tom, C. Creutz, H. Taube, *Inorg. Chem.* **1981**, *20*, 3125–3134.
[64] J. E. Sutton, H. Taube, *Inorg. Chem.* **1981**, *20*, 3125–3134.
[65] W. Kaim, K. Lahiri, W. Kaim, G. K. Lahiri, *Angew. Chem. Int. Ed.* **2007**, *46*, 1778–1796.
[66] W. Kaim, *Coord. Chem. Rev.* **2011**, *255*, 2503–2513.
[67] F. Li, J. G. Collins, F. R. Keene, *Chem. Soc. Rev.* **2015**, *44*, 2529–2542.
[68] J. A. Thomas, *Coord. Chem. Rev.* **2013**, *257*, 1555–1563.
[69] C. Creutz, H. Taube, *J. Am. Chem. Soc.* **1969**, 3988–3989.
[70] O. Impert, A. Kozakiewicz-Piekarz, A. Katafias, M. Witwicki, U. K. Komarnicka, K. Kurpiewska, R. van Eldik, *Polyhedron* **2022**, *223*, 115939.

[71] O. Impert, A. Katafias, G. Wrzeszcz, T. Muzioł, K. Hrynkiewicz, N. Olejnik, M. Chrzanowska, R. van Eldik, *J. Coord. Chem.* **2016**, *69*, 2107–2120.
[72] O. Impert, A. Katafias, P. Kita, G. Wrzeszcz, J. Fenska, G. Lente, I. Fábián, *Transit. Met. Chem.* **2011**, *36*, 761–766.
[73] T. Khan, K. Venkatasubramanian, H. C. Bajaj, Z. Shririn, *Indian J. Chem.* **1992**, *31*, 303–308.
[74] D. Chatterjee, *Coord. Chem. Rev.* **1998**, *168*, 273–293.
[75] R. E. Shepherd, H. Taube, *Inorg. Chem.* **1973**, 1392–1401.
[76] T. Matsubara, C. Creutz, *Inorg. Chem.* **1979**, *18*, 1956–1966.
[77] D. Chatterjee, M. Oszajca, A. Katafias, R. van Eldik, *Coord. Chem. Rev.* **2021**, *436*, 213773.
[78] D. Chatterjee, *New J. Chem.* **2020**, *44*, 18972–18979.
[79] T. Matsubara, C. Creutz, *J. Am. Chem. Soc.* **1978**, *100*, 6255–6257.
[80] Y. Yoshino, T. Uehiro, M. Saito, *Bull. Chem. Soc. Jpn.* **1979**, *52*, 1060–1062.
[81] H. C. Bajaj, R. van Eldik, *Inorg. Chem.* **1989**, *28*, 1980–1983.
[82] H. C. Bajaj, R. van Eldik, *Inorg. Chem.* **1990**, *29*, 2855–2858.
[83] H. C. Bajaj, R. van Eldik, *Inorg. Chem.* **1988**, *27*, 4052–4055.
[84] H. Ogino, T. Katsuyama, S. Ito, *Bull. Chem. Soc. Jpn.* **1990**, *63*, 1370–1373.
[85] D. Chatterjee, H. C. Bajaj, *J. Chem. Soc. Dalton Trans.* **1993**, 1065–1067.
[86] D. Chatterjee, H. C. Bajaj, A. Das, *J. Chem. Soc. Dalton Trans.* **1995**, 2497–2501.
[87] V. G. Povse, J. A. Olabe, *Transition Met. Chem.* **1998**, *23*, 657–662.
[88] D. Chatterjee, A. Mitra, G. S. De, *Platinum Met. Rev.* **2006**, *50*, 2–12.
[89] H. E. Toma, K. Araki, *J. Coord. Chem.* **1991**, *24*, 1–8.
[90] M. M. Taqui Khan, D. Chatterjee, H. C. Bajaj, K. N. Bhatt, S. Bhatt, S. Sanalkumar, *Indian J. Chem.* **1992**, *31*, 714–715.
[91] M. M. Taqui Khan, D. Chatterjee, H. C. Bajaj, *Indian J. Chem.* **1992**, *31*, 152–155.
[92] D. Chatterjee, K. A. Nayak, E. Ember, R. van Eldik, *Dalton Trans.* **2010**, *39*, 1695–1698.
[93] D. Chatterjee, S. Ghosh, U. Pal, *Dalton Trans.* **2011**, *40*, 683–685.
[94] D. Chatterjee, A. Mitra, M. S. A. Hamza, R. van Eldik, *J. Chem. Soc. Dalton Trans.* **2002**, 962–965.
[95] D. Chatterjee, A. Sengupta, A. Mitra, S. Basak, *Inorg. Chim. Acta* **2005**, 2954–2959.
[96] D. Chatterjee, M. S. A. Hamza, M. M. Shoukry, A. Mitra, S. Deshmukh, R. van Eldik, *Dalton Trans.* **2003**, 203–209.
[97] P. Sarkar, A. Saha, D. Chatterjee, *Transit. Met. Chem.* **2016**, *41*, 279–286.
[98] N. A. Davis, M. T. Wilson, E. Slade, S. P. Fricker, B. A. Murrer, N. A. Powell, G. R. Henderson, *Chem. Commun.* **1997**, 47–48.
[99] D. Chatterjee, S. Shome, N. Jaiswal, P. Banerjee, *Dalton Trans.* **2014**, *43*, 13596.
[100] D. Chatterjee, N. Jaiswal, P. Banerjee, *Eur. J. Inorg. Chem.* **2014**, 5856–5859.
[101] G. Ramachandraiah, *J. Am. Chem. Soc.* **1994**, *116*, 6733–6738.
[102] K. Shimizu, T. Matsubara, G. P. Sato, *Bull. Chem. Soc. Jpn.* **1974**, *47*, 1651–1656.
[103] P. G. Zanichelli, A. M. Miotto, H. F. G. Estrela, F. R. Soares, D. M. Grassi-Kassisse, R. C. Spadari-Bratfisch, E. E. Castellano, F. Roncaroli, A. R. Parise, J. A. Olabe, A. R. M. S. De Brito, D. W. Franco, *J. Inorg. Biochem.* **2004**, *98*, 1921–1932.
[104] M. M. Taqui Khan, K. Venkatasubramanian, Z. Shirin, M. M. Bhadbhade, *J. Chem. Soc. Dalton Trans.* **1995**, 1031–1035.
[105] B. T. Khan, K. Annapoorna, *Inorg. Chim. Acta* **1990**, *17*, 157–163.
[106] A. A. Diamantis, J. V. Dubrawski, *Inorg. Chem.* **1983**, *22*, 1934–1946.
[107] R. C. Rocha, F. N. Rein, H. E. Toma, *J. Braz. Chem. Soc.* **2001**, *12*, 234–242.
[108] M. M. T. Khan, A. Hussain, M. A. Moiz, *Polyhedron* **1992**, *12*, 234–242.
[109] M. Ikeda, K. Shimizu, G. P. Sato, *Bull. Chem. Soc. Jpn.* **1982**, *55*, 797–801.
[110] B. T. Khan, K. Annapoorna, *Polyhedron* **1991**, *10*, 2465–2470.
[111] B. T. Khan, K. Annapoorna, *Inorg. Chim. Acta* **1990**, *176*, 241–246.
[112] D. Chatterjee, *J. Mol. Catal (A): Chem.* **1997**, *127*, 57–60.
[113] M. M. T. Khan, D. Chatterjee, M. R. H. Siddiqui, S. D. Bhatt, H. C. Bajaj, K. Venkatasubramanian, M. A. Moiz, *Polyhedron* **1993**, *12*, 1443–1451.
[114] N. Oyama, F. A. Anson, *J. Electroanal. Chem.* **1978**, *88*, 289.
[115] N. Oyama, F. A. Anson, *J. Am. Chem. Soc.* **1979**, *101*, 1634–1635.
[116] L. Codognoto, P. G. Zanichelli, R. L. Sernaglia, *J. Braz. Chem. Soc.* **2005**, *16*, 620–625.
[117] P. G. Zanichelli, R. L. Sernaglia, D. W. Franco, *Langmuir* **2006**, *22*, 203–208.
[118] P. G. Z. Benini, B. R. McGarvey, D. W. Franco, *Nitric Oxide* **2008**, *19*, 245–251.
[119] D. Chatterjee, *J. Chem. Soc. Dalton Trans.* **1996**, 4389–4392.
[120] D. Chatterjee, *Transit. Met. Chem.* **2000**, *25*, 227–230.
[121] D. Chatterjee, N. Jaiswal, P. Sarkar, *Dalton Trans.* **2015**, *44*, 7613.
[122] D. Chatterjee, U. Pal, S. Ghosh, R. van Eldik, *Dalton Trans.* **2011**, *40*, 1302–1306.
[123] D. Chatterjee, R. van Eldik, *Macroheterocycles* **2020**, *13*, 193–20.
[124] M. Chrzanowska, A. Katafias, R. van Eldik, D. Chatterjee, *Polyhedron* **2022**, *221, 115872*.
[125] L. Sellés Vidal, C. L. Kelly, P. M. Mordaka, J. T. Heap, *Biochim. Biophys. Acta Proteins Proteomics* **2017**, *1866*, 327–347.
[126] D. Chatterjee, M. Chrzanowska, A. Katafias, R. van Eldik, *J. Inorg. Biochem.* **2021**, *225*, 111595.
[127] D. Chatterjee, R. van Eldik, *Adv. Inorg. Chem.* **2022**, *81*, 389–431.
[128] D. Chatterjee, M. Chrzanowska, A. Katafias, M. Oszajca, R. van Eldik, *RSC Adv.* **2021**, *11*, 21359–21366.

[129] C. Song, J. Zhang, in *PEM Fuel Cell Electrocatalyst: Fundamentals and Applications, Springer*, Springer, London, **2008**, pp. 89–134.
[130] D. Chatterjee, R. van Eldik, *Curr. Catal.* **2020**, *9*, 23–31.
[131] D. Chatterjee, O. Impert, R. van Eldik, *Inorg. Chem. Front.* **2023**, *10*, 1958.
[132] 'Experimental and Computational Chemistry – The Fruitful Interplay' title of a conference held in Erlangen A Symposium on the Occasion of the 65th birthday of Paul von Ragué Schleyer," **1995**.
[133] I. Alkorta, J. Elguero, J. E. Del Bene, O. Mó, M. M. Montero-Campillo, M. Yáñez, *Phys. Chem. A* **2020**, *124*, 5871–5878.
[134] I. Alkorta, M. Merced Montero-Campillo, J. Elguero, M. Yáñez, O. Mó, *Dalton Trans.* **2018**, *47*, 12516–12520.
[135] M. M. Montero-Campillo, O. Mó, M. Yáñez, I. Alkorta, J. Elguero, *Adv. Inorg. Chem.* **2019**, *73*, 73–121.
[136] M. Arrowsmith, H. Braunschweig, M. A. Celik, T. Dellermann, R. D. Dewhurst, W. C. Ewing, K. Hammond, T. Kramer, I. Krummenacher, J. Mies, K. Radacki, J. K. Schuster, *Nat. Chem.* **2016**, *8*, 890–894.
[137] G. Wang, L. A. Freeman, D. A. Dickie, R. Mokrai, Z. Benkő, R. J. Gilliard, *Chem. Eur. J.* **2019**, *25*, 4335–4339.
[138] G. Wang, J. E. Walley, D. A. Dickie, S. Pan, G. Frenking, R. J. Gilliard, *J. Am. Chem. Soc.* **2020**, *142*, 4560–4564.
[139] C. Czernetzki, M. Arrowsmith, F. Fantuzzi, A. Gärtner, T. Tröster, I. Krummenacher, F. Schorr, H. Braunschweig, *Angew. Chem. Int. Ed.* **2021**, *133*, 20944–20948.
[140] J. L. Dutton, G. Frenking, *Angew. Chem. Int. Ed.* **2016**, *55*, 13380–13382.
[141] B. Rösch, T. X. Gentner, J. Eyselein, J. Langer, H. Elsen, S. Harder, *Nature* **2021**, *592*.
[142] B. Rö, S. Harder, *Chem. Commun.* **2021**, *57*, 9354.
[143] M. Gimferrer, S. Danés, E. Vos, C. B. Yildiz, I. Corral, A. Jana, P. Salvador, D. M. Andrada, *Chem. Sci.* **2022**, *13*, 6583–6591.
[144] S. Pan, G. Frenking, *Chem. Sci.* **2022**, *14*, 379–383.
[145] M. Gimferrer, S. Danés, E. Vos, C. B. Yildiz, I. Corral, A. Jana, P. Salvador, D. M. Andrada, *Chem. Sci.* **2023**, 384–392.
[146] R. J. F. Berger, S. Jana, R. Fröhlich, N. W. Mitzel, *Z. Naturforsch. B* **2011**, *66*, 1131–1135.
[147] R. J. F. Berger, S. Jana, R. Fröhlich, N. W. Mitzel, *Z. Naturforsch. B* **2015**, *70*, 279–282.
[148] M. R. Buchner, D. Ćoćić, S. I. Ivlev, N. Spang, M. Müller, R. Puchta, *Dalton Trans.* **2023**, *52*, 5287.
[149] D. F. Bekiş, L. R. Thomas-Hargreaves, C. Berthold, S. I. Ivlev, M. R. Buchner, *Z. Naturforsch. B* **2023**, *78*, e202200347.
[150] L. R. Thomas-Hargreaves, Y. Q. Liu, Z. H. Cui, S. Pan, M. R. Buchner, *J. Comput. Chem.* **2023**, *44*, 397–405.
[151] L. R. Thomas-Hargreaves, C. Berthold, W. Augustinov, M. Müller, S. I. Ivlev, M. R. Buchner, *Chem. Eur. J.* **2022**, *28*.
[152] M. R. Buchner, N. Spang, S. I. Ivlev, *Z. Naturforsch. B* **2022**, *77*, 381–390.
[153] L. R. Thomas-Hargreaves, S. Pan, S. I. Ivlev, G. Frenking, M. R. Buchner, *Inorg. Chem.* **2022**, *61*, 700–705.
[154] J. K. Buchanan, R. J. Severinsen, M. R. Buchner, L. R. Thomas-Hargreaves, N. Spang, K. D. John, P. G. Plieger, *Dalton Trans.* **2021**, *50*, 16950–16953.
[155] M. R. Buchner, *Chem. Eur. J.* **2019**, *25*, 12018–12036.
[156] M. Biruš, A. Budimir, M. Gabricevič, *J. Inorg. Biochem.* **1999**, *75*, 85–91.
[157] W. Petz, K. Dehnicke, B. Neumüller, *Z. Anorg. Allg. Chem.* **2011**, *637*, 1761–1768.
[158] W. Petz, K. Dehnicke, N. Holzmann, G. Frenking, B. Neumüller, *Z. Anorg. Allg. Chem.* **2011**, *637*, 1702–1710.
[159] R. Puchta, B. Neumüller, K. Dehnicke, *Z. Anorg. Allg. Chem.* **2011**, *637*, 67–74.
[160] B. Neumüller, K. Dehnicke, *Z. Anorg. Allg. Chem.* **2010**, *636*, 1516–1521.
[161] B. Neumüller, K. Dehnicke, *Z. Anorg. Allg. Chem.* **2010**, *636*, 438–1440.
[162] G. Frenking, N. Holzmann, B. Neumüller, K. Dehnicke, *Z. Anorg. Allg. Chem.* **2010**, *636*, 1772–1775.
[163] F. Kraus, M. B. Fichtl, S. A. Baer, *Z. Naturforsch.* B **2009**, *64*, 257–269.
[164] D. Naglav, M. R. Buchner, G. Bendt, F. Kraus, S. Schulz, *Angew. Chem. Int. Ed.* **2016**, *55*, 10562–10576.
[165] F. Dankert, H. L. Deubner, M. Müller, M. R. Buchner, F. Kraus, C. von Hänisch, *Z. Anorg. Allg. Chem.* **2020**, *646*, 1–8.
[166] F. Kraus, S. A. Baer, M. R. Buchner, A. J. Karttunen, *Chem. Eur. J.* **2012**, *18*, 2131–2142.
[167] M. Schmidt, A. Bauer, H. Schmidbaur, *Inorg. Chem.* **1997**, *36*, 2040–2043.
[168] M. P. Dressel, S. Nogai, R. J. F. Berger, H. Schmidbaur, *Z. Naturforsch. B* **2003**, *58*, 173–182.
[169] R. J. F. Berger, M. Hartmann, P. Pyykkö, D. Sundholm, H. Schmidbaur, *Inorg. Chem.* **2001**, *40*, 2270–2274.
[170] R. J. F. Berger, M. Schmidt, J. Juselius, D. Sundholm, P. Sirsch, H. Schmidbaur, *Z. Naturforsch. B* **2001**, *56*, 979–989.
[171] R. J. F. Berger, M. A. Schmidt, J. Jusélius, D. Sundholm, P. Sirsch, H. Schmidbaur, *Z. Naturforsch. B* **2001**, *58*, 173.
[172] D. Dange, A. Paparo, C. Jones, *Chem. Asian J.* **2020**, *15*, 2447–2450.
[173] A. Paparo, C. D. Smith, C. Jones, *Angew. Chem. Int. Ed.* **2019**, *58*, 11459–11463.
[174] O. Raymond, M. Bühl, J. R. Lane, W. Henderson, P. J. Brothers, P. G. Plieger, *Inorg. Chem.* **2020**, *59*, 2413–2425.
[175] P. G. Plieger, K. D. John, T. S. Keizer, T. M. McCleskey, A. K. Burrell, R. L. Martin, *J. Am. Chem. Soc.* **2004**, *126*, 14651–14658.
[176] R. J. F. Berger, R. Mera-Adasme *Z. Naturforsch. B* **2016**, *71*, 71–75.
[177] M. D. Rossman, M. B. Powers, O. P. Preuss, *Beryllium: Biomedical and Environmental Aspects*, Williams & Wilkins, Philadelphia, **1991**.
[178] R. J. F. Berger, P. Håkansson, R. Mera-Adasme, *Z. Naturforsch. B* **2020**, *75*, 413–419.
[179] J. Elguero, I. Alkorta, *Struct. Chem.* **2023**, *34*, 391–398.
[180] L. B. Tepper, Harriet L. Hardy, R. I. Chamberlin, *Toxicity of Beryllium Compounds.*, Elsevier Publishing Company, **1961**.
[181] Jochen Jander, Ch Lafrenz, *Wasserähnliche Lösungsmittel*, Verlag Chemie, **1968**.
[182] S. F. Lincoln, M. N. Tkaczuk, *Ber. Bunsenges. Phys. Chem.* **1981**, *85*, 433–437.

[183] S. F. Lincoln, M. N. Tkaczuk, *Ber. Bunsenges. Phys. Chem.* **1982**, *86*, 221–225.
[184] P. A. Pittet, G. Elbaze, L. Helm, A. E. Merbach, *Inorg. Chem.* **1990**, *29*, 1936–1942.
[185] F. A. Dunand, L. Helm, A. E. Merbach, *Adv. Inorg. Chem.* **2003**, *54*, 1.
[186] R. van Eldik, C. D. Hubbard, in *Chemistry at Extreme Conditions*, Elsevier, Amsterdam, **2005**.
[187] T. W. Swaddle, *Inorg. Chem.* **1983**, *22*, 2663.
[188] R. Puchta, M. Galle, N. van Eikema Hommes, E. Pasgreta, R. van Eldik, *Inorg. Chem.* **2004**, *43*, 8227–8229.
[189] E. Pasgreta, R. Puchta, A. Zahl, R. van Eldik, *Eur. J. Inorg. Chem.* **2007**, *2007*, 1815–1822.
[190] E. Pasgreta, R. Puchta, M. Galle, N. van Eikema Hommes, A. Zahl, R. van Eldik, *ChemPhysChem* **2007**, *8*, 1315–1320.
[191] R. Puchta, N. J. R. van Eikema Hommes, R. van Eldik, *Helv. Chim. Acta* **2005**, *88*, 911–922.
[192] A. Budimir, M. Walther, R. Puchta, R. van Eldik, *Z. Anorg. Allg. Chem.* **2011**, *637*, 515–522.
[193] H. Elsen, R. Puchta, *in preparation.* **2023**.
[194] M. Walther, A. Budimir, R. Puchta, *J. Coord. Chem.* **2012**, *65*, 4359–4374.
[195] R. Puchta, R. van Eldik, *Helv. Chim. Acta* **2008**, *91*, 1063–1071.
[196] M. Walther, R. Puchta, *RSC Adv.* **2012**, *2*, 5815.
[197] R. Puchta, R. van Eldik, *Inorg. Chem.* **2004**, *43*, 8227–8829.
[198] R. Weiss, F. Pühlhofer, N. Jux, K. Merz, *Angew. Chem.* **2002**, *114*, 2696–2971.
[199] F. P. Rotzinger, *J. Am. Chem. Soc.* **1996**, *118*, 6760–6766.
[200] F. P. Rotzinger, *J. Am. Chem. Soc.* **1997**, *119*, 5230–5238.
[201] A. Mijatović, B. Šmit, A. Rilak, B. Petrović, D. Čanović, Ž. D. Bugarčić, *Inorg. Chim. Acta* **2013**, *394*, 552–557.
[202] A. M. Mijatović, R. M. Jelić, J. Bogojeski, Ž. D. Bugarčić, B. Petrović, *Monatsh. Chem.* **2013**, *144*, 1489–1498.
[203] A. Rilak, I. Bratsos, E. Zangrando, J. Kljun, I. Turel, Ž. D. Bugarčić, E. Alessio, *Inorg. Chem.* **2014**, *53*, 6113–6126.
[204] H. Huang, P. Zhang, Y. Chen, L. Ji, H. Chao, *Dalton Trans.* **2015**, *44*, 15602–15610.
[205] H. Huang, P. Zhang, Y. Chen, K. Qiu, C. Jin, L. Ji, H. Chao, *Dalton Trans.* **2016**, *45*, 13135–13145.
[206] M. Međedović, A. Rilak Simović, D. Ćoćić, L. Senft, S. Matić, D. Todorović, S. Popović, D. Baskić, B. Petrović, *Dalton Trans.* **2023**, *52*, 1323–1344.
[207] M. Medjedović, A. R. Simović, D. Ćoćić, M. Milutinović, L. Senft, S. Blagojević, N. Milivojević, B. Petrović, *Polyhedron* **2020**, *178*, 114334.
[208] S. Betanzos-Lara, A. Habtemariam, P. J. Sadler, *J. Mex. Chem. Soc.* **2013**, *57*, 160.
[209] Z. Liu, I. Romero-Canelón, B. Qamar, J. M. Hearn, A. Habtemariam, N. P. E. Barry, A. M. Pizarro, G. J. Clarkson, P. J. Sadler, *Angew. Chem. Int. Ed.* **2014**, *126*, 4022–4027.
[210] J. J. Soldevilla-Barreda, I. Romero-Canelon, A. Habtemariam, P. J. Sadler, *Nat. Commun.* **2015**, *6*, 6582.
[211] S. Kern, R. van Eldik, *Inorg. Chem.* **2012**, *51*, 7340–7345.
[212] K. J. Takeuchi, M. S. Thompson, D. W. Pipes, T. Meyer, *Inorg. Chem.* **1984**, *23*, 1845–1851.
[213] J. J. Concepcion, J. W. Jurss, J. L. Templeton, T. J. Meyer, *J. Am. Chem. Soc.* **2008**, *130*, 16462–16463.
[214] H.-W. Tseng, R. Zong, J. T. Muckerman, R. Thummel, *Inorg. Chem.* **2008**, *47*, 11763–11773.
[215] S. Masaoka, K. Sakai, *Chem. Lett.* **2009**, *38*, 182–183.
[216] D. J. Wasylenko, C. Ganesamoorthy, B. D. Koivisto, M. A. Henderson, C. P. Berlinguette, *Inorg. Chem.* **2010**, *49*, 2202–2209.
[217] D. J. Wasylenko, R. D. Palmer, C. P. Berlinguette, *Chem. Commun.* **2013**, *49*, 218–227.
[218] J. D. Blakemore, R. H. Crabtree, G. W. Brudvig, *Chem. Rev.* **2015**, *115*, 12974–13005.
[219] D. Jaganyi, A. Hofmann, R. van Eldik, *Angew. Chem. Int. Ed.* **2001**, *40*, 1680–1683.
[220] A. Hofmann, D. Jaganyi, O. Q. Munro, G. Liehr, R. van Eldik, *Inorg. Chem.* **2003**, *42*, 1688–1700.
[221] A. Hofmann, L. Dahlenburg, R. van Eldik, *Inorg. Chem.* **2003**, *42*, 6528–6538.
[222] B. Petrović, Ž. D. Bugarčić, A. Dees, I. Ivanović-Burmazović, F. W. Heinemann, R. Puchta, S. N. Steinmann, C. Corminboeuf, R. van Eldik, *Inorg. Chem.* **2012**, *51*, 1516–1529.
[223] D. Ćoćić, M. Chrzanowska, A. Katafias, R. Puchta, R. van Eldik, *J. Coord. Chem.* **2021**, *74*, 433–443.
[224] M. Chrzanowska, A. Katafias, O. Impert, A. Kozakiewicz, A. Surdykowski, P. Brzozowska, A. Franke, A. Zahl, R. Puchta, R. van Eldik, *Dalton Trans.* **2017**, *46*, 10264–10280.
[225] L. Helm, A. E. Merbach, *Chem. Rev.* **2005**, *105*, 1923–1959.
[226] M. Chrzanowska, A. Katafias, A. Kozakiewicz, R. Puchta, R. van Eldik, *J. Coord. Chem.* **2018**, *71*, 1761–1777.
[227] D. Ćoćić, B. Petrović, R. Puchta, M. Chrzanowska, A. Katafias, R. van Eldik, *J. Comput. Chem.* **2022**, *43*, 1161–1175.
[228] S. Liu, *Conceptual Density Functional Theory*, WILEY-VCH GmbH, Boschstr. 12, 69469 Weinheim, Germany, **2022**.

Manuscript received: August 16, 2023
Revised manuscript received: September 22, 2023
Version of record online: ■■ ■■, ■■■■

PERSONAL ACCOUNT

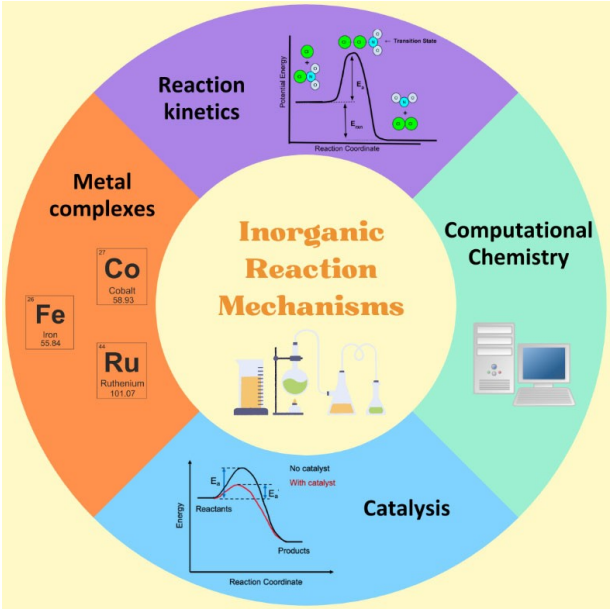

*J. Polaczek, K. Kieca, M. Oszajca, O. Impert, A. Katafias, D. Chatterjee, D. Ćoćić, R. Puchta, G. Stochel, C. D. Hubbard, R. van Eldik**

1 – 32

A Personal Account on Inorganic Reaction Mechanisms

The manuscript presents the research in the field of coordination chemistry involving the interaction of small molecules with microperoxidase and cobalamin. Characterization of mixed-valence Ru(II)/Ru(III) ion-pair complexes; electrochemistry, redox-reactions and catalytic significance of $Ru^{III/II}$(edta) complexes, as well as mechanistic information from DFT studies.